

Title:

Elucidating the role of intrinsic adenosine A1 receptors in acute alcoholism using human induced pluripotent stem cell-derived hepatocytes

Authors:

Takako Nagata^{1*} & Yuning George Huang²

Affiliations:

¹NT Biologics, Gaithersburg, MD, USA

²National Institute of Diabetes and Digestive and Kidney Diseases, National Institutes of Health, Bethesda, MD, USA

Corresponding author:

Takako Nagata, takako@nt-biologics.com

Abstract

Acute alcoholic hepatitis (AAH) from binge drinking is a serious disease. It is associated with a high mortality rate, especially among young adults. Apoptosis is known to be a primary cause of liver damage, and it can be induced by either intrinsic signaling pathways or by reactive oxygen species (ROS). Adenosine A1 receptors (ADORA1) are known to be involved in ethanol metabolism; however, underlying mechanism is not well understood. For investigating how the intrinsic ADORA1 function in ethanol metabolism in normal human hepatocytes without interference by extrinsic molecules, primary hepatocytes pose a challenge, due to unavoidable contamination by other kinds of cells in the liver. Also, they are difficult to culture stably. As a novel alternative, hepatocytes derived from human induced pluripotent stem cells were employed, because they display similar function to primary hepatocytes and they can be stably cultured. The dynamics and integrity of signal transduction mechanisms were investigated by following chronological changes in gene expression. This shed light on how and when the ADORA1 function and on causal relationships between the pathways and clinical symptoms. The findings of this study shows that ADORA1 are most activated soon after exposure to ethanol, and transfection of small interfering RNA targeting ADORA1-messenger-RNA (ADORA1-siRNA) into the hepatocytes significantly suppresses production of actin protein and ROS. It suggests that ADORA1 in the liver contribute to apoptosis in acute alcoholism through both intrinsic pathway and ROS activity. Also, actin that is abundant in the cells could be an appropriate biomarker evaluating hepatic function status.

Introduction

Acute alcoholism from binge drinking has been a persistent problem worldwide. It especially targets youth, and the significantly high mortality rate destroy families while sacrificing lifetimes of human potential. So far, radical treatments have not been established and palliative therapies are sadly the rule. Moreover, alcohol induced acute hepatitis is often followed by fulminant hepatitis, where one-month mortality rates are 40 to 50 (1) %. According to the Centers for Disease Control and Prevention in the United States, during 2015–2019, excessive alcohol use was responsible on average for more than 140,000 deaths annually. More than 40% were tied to binge drinking.

Adenosine receptors are widely distributed and play vital roles in our bodies. Their expression is highly varied in each organ. Expression of adenosine A1 receptors (ADORA1), is highest in neurons; while the liver displays far lower expression — one of the lowest among tissues. Still, it was reported that ADORA1 plays a role in increasing ethanol-mediated hepatic steatosis by activating hepatic stellate cells (2).

Reactive oxygen species (ROS) are known to increase under oxidative stress and to cause apoptosis independently from caspase3 involved pathways. Hence, accumulation of ROS in response to inflammation should also facilitate apoptosis. Induced apoptosis results in damage to nucleic acids, proteins, and membrane lipids in pathological conditions such as alcoholic hepatitis.

Hepatocytes exposed to sudden toxic concentrations of ethanol are subject to apoptosis via both intrinsic (mitochondria-mediated) and extrinsic (receptor-mediated) pathways. Hence, we investigated how ADORA1 contributes to ethanol metabolism, using HepG2 human hepatoma cell lines and ADORA1 knockout mice. Treatment of hepatocytes with ethanol in rats induces activation of c-Jun N-terminal kinase (3) that, in turn, activates some caspases which are pro-apoptotic enzymes. Caspase 3 is known to be typical among them and its activation level clearly reflects the severity of apoptosis.

The results (Figure S1 in Supporting information) were officially presented as poster 294 at the 35th Annual Scientific Meeting of the Research Society on Alcoholism in 2012 (4). In summary, ADORA1 apparently plays a robust role in the upregulation of ethanol metabolism in hepatocytes both in intrinsic and extrinsic pathways despite its low expression in the liver. As caspase3 is activated in both pathways, in order to figure out to which pathway(s) ADORA1 contributes in normal human hepatocytes following ethanol surge, primary hepatocytes were considered. However, it is technically challenging to isolate hepatocytes from other types of cells in liver, and to stably culture them. Hepatocytes derived from human induced pluripotent stem cells (iPSC) were employed in this study to exclude the possibility of contamination, and also because they are stable in culture.

The RNA interference (RNAi) system downregulates specific gene expressions by double-stranded RNA (5). Following this discovery, it was reported that synthetic small interfering RNA (siRNA) could induce RNA-interference in mammalian cells (6).

In this study, the kinetics of gene expression both in RNA and protein was investigated following exposure to a high concentration of ethanol in order to elucidate mechanisms where ADORA1, acts as a key molecule ethanol-induced metabolism associated with apoptosis, and in order to identify symptoms of acute alcoholic hepatitis that individual molecules and their involved pathways contribute to. Simultaneously, small interfering RNA targeting ADORA1-messenger-RNA (ADORA1-siRNA) was examined to see whether it suppresses the effects of ADORA1 in ethanol-induced cascades. ROS assay was also performed in order to verify this suppressive effect of ADORA1-siRNA.

Materials and methods

Reagents

Small interfering RNAs (siRNAs) to ADORA1, GAPDH, and Negative Control were purchased from Ambion (Austin, TX, USA). Lipofectamin (Lipofectamine RNAiMAX) was purchased from Invitrogen (Carlsbad, CA, USA). Tween20 and bovine serum albumin-fraction V (BSA) were purchased from RPI (Mount Prospect, IL, USA). Rabbit anti-ADORA1 antibody was purchased from Sigma-Aldrich (Saint Louis, MO, USA). Mouse anti-actin antibody was purchased from Proteintech (Rosemont, IL, USA). Mouse anti-caspase 3, and anti-GAPDH antibodies were purchased from Santa Cruz Biotechnology (Dallas, TX, USA). Goat anti-rabbit Poly-HRP and goat anti-mouse IgG (H+L) Poly-HRP secondary antibodies were purchased from Invitrogen. Pre-casted 4–20% gradient gels, polyvinylidene fluoride (PVDF) membrane and other laboratory reagents were purchased from Bio-Rad (Hercules, CA, USA).

Cell culture

Human hepatocytes derived from the Cellartis human induced pluripotent stem cell line 18 (ChiPSC18) were seeded and cultured at 1×10^5 / well and 150ul / well in 96 well plates with hiPS-HEP Medium (the Cellartis® Enhanced hiPS-HEP v2 Kit) according to its user manual (Takara Bio Europe AB, Sweden, catalog # Y10134). This cell line was derived from skin fibroblasts from a healthy volunteer (81kg/175cm), a 32-year-old adult male human (European/North African). HLA typification data: HLA-A*23:01; HLA-B*07:02, HLA-B*49:01; HLA-C*07:01, HLA-C*07:02; HLA-DRB1*04:06, HLA-DRB1*07:01; HLA-DQB1*02:02, HLA-DQB1*04:02; HLA-DPB1*03:01, HLA-DPB1*04:01.

ADORA1-siRNA transfection into hepatocytes

During the second week of culture, the cells were cultured with or without ethanol 100mM. ADORA1-siRNA was independently transfected into the hepatocytes with Lipofectamine RNAiMAX Reagent (Invitrogen) according to manufacturer's protocol (Silencer Select siRNAs).

Total RNA isolation and quantitative PCR

The hepatocytes cultured for 1.5, 3, or 6 hours after the addition of ethanol were readily dissolved in TRIzol (Invitrogen) after the harvest and total RNA was purified according to the manufacturer's instructions using RNA Clean & Concentrator-5 (Zymo Research, Irvine, CA, USA). The total RNA was quantified by Qubit 4 Fluorometer (Thermo Fisher Scientific, Waltham, MA, USA) and RNA integrity was assessed by 4150 TapeStation instrument G2992A (Agilent, Santa Clara, CA, USA). cDNA was generated on MyCycler (Bio-Rad) using Oligo(dT)20 Primer (Invitrogen) following manufacturer's instructions. The cDNA was subjected to quantitative real-time PCR with PowerUp SYBR Green Master Mix (Applied Biosystems, Thermo Fisher Scientific) on 7500 Real-Time PCR System (Applied Biosystems). The sequences of the PCR oligonucleotide primers are listed in Table 2. The quantitative PCR experiments were repeated at least three times.

Next Generation Sequencing (NGS) for gene expressions

Total RNAs obtained above were sent to Novogene (Beijing, China) which prepared RNA library and transcriptome sequencing using Illumina NovaSeq 6000. Differential gene expression was then calculated with DESeq2. Genes with adjusted p-value < 0.05 and $|\log_2(\text{FoldChange})| > 0$ were considered to be differentially expressed. The reference genome was Homo Sapiens (GRCh38/hg38). The data obtained were analyzed using NovoSmart (Novogene) developed based on R shiny, Excel, Cytoscape, UniProt, and KEGG PATHWAY Database.

Western blotting

The hepatocytes cultured for 2 days after the addition of ethanol were harvested and their cell pellets underwent the procedures as previously described in detail (7). Protein concentrations were measured by Qubit 4 Fluorometer (Thermo Fisher Scientific) and by NI™ (Non-Interfering™) Protein Assay Kit (G-Biosciences, St Louis, Missouri, USA). Protein samples reduced with β -mercaptoethanol at 3% (Sigma Aldrich) (around 30ug for ADORA1 and actin, 20ug for caspase 3) were loaded per lane on 4–20% gradient gels (Bio-Rad) along with rainbow markers (Amersham, Buckinghamshire, UK). Gels were run cold at constant 90 volts for an hour and a half. The separated proteins were transferred cold onto polyvinylidene fluoride (PVDF) membrane (Bio-Rad) at constant 300~350 mA for around 1.5 hr. The membranes were blocked for 1 hr in blocking buffer (3% BSA-PBS) on an orbital shaker (Benchmark, Tempe, AZ, USA) at ambient temperature. Following this, the membranes were incubated in PBS with Tween 20 at 0.1% (PBST) containing each one of the primary Abs (anti-ADORA1 diluted to 1:1000, anti-GAPDH diluted to 1:100, anti-actin diluted to 1:16000, and anti-caspase 3 diluted to 1:200) at 6 degrees overnight. Following this, each membrane was washed four times

for four minutes each in a washing buffer (0.1% Tween 20 in PBS). To enhance signals, poly-HRP conjugated secondary antibodies were employed (Mishra et al., 2019). Next, the membrane was incubated for one hour with each one of the secondary antibodies (goat anti-rabbit PolyHRP and goat anti-mouse IgG (H+L) Poly-HRP) at 1:10000 dilution in 1% fat-free-milk PBST on the orbital shaker at ambient temperature. The incubated membranes were washed four times for four minutes each in washing buffer (Tween 20 at 0.1% in PBS), and developed with ECL Prime (Amersham). The fluorescence of the membrane bands was quantified by measuring their total fluorescence signals and analyzed using Amersham Imager 680 and ImageQuant TL (GE Healthcare, Chicago, IL, USA). The western blot experiments were repeated at least three times.

ROS assay

The hepatocytes were cultured at 1×10^5 / well and 150ul / well in black, clear-bottom, tissue culture-treated 96-well plates (Corning, Corning, NY, USA). First, the plates were added 50 μ l/well using cold Hepatocyte Coating in Cellartis Enhanced hiPS-HEP Thawing and Plating Kit (Takara Bio Europe AB, catalog # Y10132), then incubated at room temperature for 60 min. Following removal of the Hepatocyte Coating from the wells just before seeding, the cultured cells were subjected to Dihydroethidium (hydroethidine or DHE) based ROS assay, according to manufacturer's protocol (Cayman Chemical, Ann Arbor, MI, USA). The hepatocytes were cultured for 3 or 48 hours at 100mM of ethanol with or without the addition of ADORA1-siRNA. Antimycin A was used as the positive control and N-acetyl cysteine as the negative control. The fluorescence was measured using an exciting wave length of 485nm and an emission wave length of 590nm by SPECTRAMAX GEMINIEM Microplate Reader (Molecular Devices, San Jose, CA, USA). Data was analyzed by SoftMax Pro Software (Molecular Devices). In Figure 4B, the Y-axis is absorbance, where the scale was determined by the positive and negative controls. The ROS assay was repeated at least three times

Morphology

Hepatocytes were cultured for 46hr with or without 100mM of ethanol, and with 100mM of ethanol and ADORA1-siRNA. Images were taken directly on hepatocyte-cultured plates using Leica DMI1 (phase-contrast microscope) and MC120 HD (camera), and analyzed using Leica Application Suite.

Statistical analysis

All data are presented as the mean \pm SEM. Statistical significance was determined by t test or ANOVA.

Results

Chronological changes in gene expression at both mRNA and protein levels

The kinetics of signal transduction cascades induced by ethanol were examined using quantitative real time PCR and western blotting. Figure 1 shows quantitative-real-time-PCR (qPCR) results showing chronological, ethanol induced changes at the mRNA level of ADORA1 (Figure 1A) and caspase 3 (Figure 1B) in iPSC derived hepatocytes which were cultured up to 6 hours, along with ethanol stimulation at 100mM. Figure 1A shows that ADORA1 mRNA levels peaked at 1.5hr after administering ethanol, trending down from 1.5hr to 6hr. Meanwhile, caspase 3 peaked at 3hr (Figure 1B). For the protein expression levels, normalization was performed with GAPDH (Figure 2). Across the analyzed samples, GAPDH expression had been consistently high and stable, and much stronger than the other measured molecules. As a result, the observed minor variations in GAPDH levels across the time course should not affect GAPDH to serve as the housekeeping gene and the internal control. Furthermore, normalization with total loaded protein was also performed, ensuring that obtained normalized values are reliable (Figure S2). In Fig. 2A, protein expressions not only of ADORA1 but also of actin were notably upregulated. In Fig. 2B, caspase 3 protein expression was upregulated as well.

Signal transduction mechanisms and kinetics

Samples were taken at 0 (control), 1.5, 3 and 6hr in the time course of culture with 100mM of ethanol, then subject to Next Generation Sequencing. Figure 3A is the heatmap comparing each time point. Table S1 in Supporting information is a list of expressed gene symbols and names in the same order that they appear on the heatmap. The map shows that the inactivated area in the control got activated and the activated area in control became silent after adding ethanol, and there are clusters of molecules particularly activated at each time point. Figure 3B, 3C, and 3D are diagrams of gene-expressed proteins at 1.5, 3 and 6hr. Table 1 summarizes major genes/proteins expressed in response to ethanol stimulation. Most gene expression appeared at specific time points. However, some proteins were expressed at all three time points:

- CYP2E1 (cytochrome P450 monooxygenase) and ADH1 (alcohol dehydrogenase) were notably activated.
- HABP2 (Hyaluronan-binding protein 2), which is a coagulation factor VII-activating serine protease, was very highly activated.(9–11)
- ACTA1 (Actin, alpha 1) showed strong upregulation at all three time points, although it is accompanied by two other molecules that appeared at only one of the three time points. CDC42BPG (CDC42-binding protein kinase gamma) was mildly upregulated only at 1.5hr (Fig. 3B), and ARHGEF26 (Rho guanine nucleotide exchange factor 26) only at 6hr (Fig. 3D).

- NOXA1 (A superoxide- producing NADPH oxidase), which induces the production of reactive oxygen species (ROS), was also mildly upregulated.

Moreover, some molecules were activated mainly at 6hr (Fig. 3D):

- ID1 (DNA-binding protein inhibitor ID-1) was very highly activated. ID1 positively regulates actin filament bundle assembly and apoptosis (12).
- DDIT4 (DNA damage-inducible transcript 4 protein) is significantly upregulated. DDIT4 induces p53/TP53-mediated apoptosis by inhibiting the activity of the “mammalian target of rapamycin complex 1” (mTORC1), and is activated in response to cellular stress including DNA damage (13).
- OXT (oxytocin-neurophysin 1) was strongly upregulated. OXT is a prepropeptide which is cleaved into the two chains – oxytocin and neurophysin I. High concentrations of oxytocin inhibit the growth of liver (14). Oxytocin also upregulates prostaglandin secretion.

Furthermore, PTGDR2 (Prostaglandin D2 receptor 2) was mildly activated at 1.5 and 6hr (Fig 3B and 3D). This receptor's activation is involved in inflammation responses. Also, KNG1 (Kininogen-1) is mildly upregulated at 1.5hr (Fig. 3B). It plays an important role in blood coagulation and functions as a mediator of inflammatory response including release of prostaglandins.

Meanwhile, quite a few molecules remained suppressed after ethanol administration (Fig. 3):

- SLC2A1 (solute carrier family 2, facilitated glucose transporter member 1) was remarkably repressed, causing glucose uptake to be signally reduced;
- LYZ (Lysozyme C) was remarkably repressed. More than 10% of cellular glycogen is located within the lysosome, which becomes a final energy source in stress situations including starvation with the rupture of lysosomes (15). LYZ repression is proposed to accelerate the aggravation of starvation of hepatocytes, as this final energy store becomes much less available despite in the starvation state.
- IGFBP1 (Insulin-like growth factor binding protein 1) was strikingly repressed, leading to downregulation of glucose uptake and unequivocal facilitation of programmed cell death, as IGF-1 is one of the most potent activators of the AKT signaling pathway (16).
- SERPINE1 — serpin peptidase inhibitor, clade E (nexin, plasminogen activator inhibitor type 1), member 1 — was strongly downregulated. In the presence of vitronectin (VTN), SERPINE1 was found to be an effective thrombin inhibitor (17). In this study, VTN was significantly upregulated at 1.5hr, possibly due to positive feedback brought about by the downregulation of SERPINE1. SERPINE1 interacts with IGFBP1 signaling from SERPINE1 to IGFBP1. It seems that the downregulation of SERPINE1 intensifies the downregulation of IGFBP1.

Moreover, CEBPB (CCAAT/enhancer binding protein (C/EBP), beta) showed very strong repression at 3 and 6hr (Fig. 3C and D), especially at 6hr. This molecule plays a significant role in the gluconeogenic pathway and in the regulation of acute-phase

reaction and inflammation. Therefore, CEBPB repression should significantly reduce gluconeogenesis, leaving hepatocytes with much less available glucose and more aggressive inflammation.

PHLDA2 (Pleckstrin homology-like domain family A member 2) was moderately downregulated at 3hr and 6hr (Fig. 3C and 3D). It controls glycogen storage (18).

Here, PHLDA2 downregulation together with LYZ, play an important role in glycogen storage and suppression of glycogenolysis, worsening the starvation state.

SOAT2 (sterol O-acyltransferase 2: cholesterol acyltransferase 2) was markedly downregulated at 3hr (Fig. 3C). It produces intracellular cholesterol esters for lipoprotein secretion from hepatocytes (19). Therefore, its downregulation seems to induce the retention of lipids inside the hepatocytes. Moreover, GK (ATP:glycerol 3-phosphotransferase) was significantly suppressed at 3 and 6hr (Fig. 3C and 3D). This is a key enzyme in the regulation of glycerol uptake.

IER3 (Radiation-inducible immediate-early gene IEX-1) was moderately suppressed at 3 hr (Fig. 3C). ERK1/2 is activated by IER3 (20–22). CTGF (synonym of CCN2, CCN family member 2) was significantly suppressed at 3 and 6hr (Fig. 3C and 3D). This molecule positively regulates the cascades of ERK1 and ERK2 as well as JNK.

Use of actin as a damage marker and the role of ADORA1 in alcohol-intoxicated hepatocytes using ADORA1-siRNA

Actin is known as one of the most abundant proteins in hepatocytes. Therefore, changes in actin expression levels were anticipated to be more apparent than those of other proteins. In Figure 4A, hepatocytes transfected with ADORA1-siRNA exhibited a significant downregulation of actin protein expression after 48 hours of culture in 100 mM ethanol, compared to cells cultured only in 100 mM ethanol for the same duration. Figure 4B shows the results of a ROS assay under the same conditions as Figure 4A. ROS production was significantly higher at 48 hours than at 3 hours of incubation with 100mM of ethanol. However, the amount of ROS was significantly lower in the ADORA1-siRNA transfected hepatocytes at both 3 hours and 48 hours. For morphologic analysis of the hepatocytes, images were taken using a phase-contrast light microscope (Fig. 4C). Apoptotic bodies and lipid droplets were visible in the cells that were cultured in ethanol for 46 hours (Figure 4C-b). These abnormalities were less discernible in the cells that were transfected with ADORA1-siRNA (Figure 4C-c). No such abnormalities were seen in the cells that were cultured in medium only (Figure 4C-a). These findings suggest that blocking ADORA1 with siRNA can reduce the production of ROS and apoptosis in the hepatocytes cultured with ethanol; and that actin can be used as a biomarker of damage in alcohol-intoxicated hepatocytes.

Discussion

The findings of this study demonstrated that massive ethanol influx into hepatocytes causes a variety of complex reactions. CYP2E1 is a membrane protein expressed in hepatocytes acting as the gateway for ethanol to enter the cascade. It has been reported that transcriptional induction of CYP2E1 occurs with high levels of ethanol (23). Interestingly, another protein, NOXA1 was readily activated along with CYP2E1 in response to ethanol stimulation, and remained activated at all three time points. This correlates well with the rapid elevation of ROS production brought about by the surge of a toxically high concentration of ethanol (Fig. 4C).

CDC42BPG is a serine/threonine-protein kinase, and ARHGEF26 activates Rho GTPase by promoting the exchange of GDP for GTP. Cdc42 is a GTPase of the Rho family involved in various signaling pathways which controls diverse cellular functions, including actin assembly and rearrangement. It is known that actin is upregulated in response to stresses and form stress fibers (24). Therefore, CDC42BPG and ARHGEF26 acting together are postulated to activate actin formation. ID1 is assumed to boost actin accumulation.

DDIT4 is activated in response to many stress stimuli including DNA damage. Therefore, it is proposed that DDIT4 upregulation was induced at the later time point through apoptosis accompanying DNA damage, and through stresses from starvation and inflammation by the rapid influx of the high concentration of ethanol. In turn, ID1 upregulation induces apoptosis through an intrinsic (mitochondria-mediated) pathway (KEGG apoptosis pathway: <https://www.genome.jp/pathway/hsa04210>). Thus, once the cycle of this sequence is established, apoptosis is assumed to rapidly accelerate, predisposing the hepatocytes to fulminant and fatal hepatitis. Hence, a number of stresses triggered by the ethanol surge are likely to have induced DDIT4 and ID1 upregulation observed at the later time point.

In this study, an acute and high rise in the concentration of ethanol forced hepatocytes to suffer from increasingly low levels of glucose, brought about by the various described molecules related to this ethanol surge. This surge is postulated to starve hepatocytes thus effectively and hence further aggravate inflammation and apoptosis. Also, both IER3 and CTGF suppression are postulated to synergistically facilitate apoptosis by the downstream suppression of MAP kinase pathways.

In the meantime, it is known that acute hepatitis accompanies steatosis (25). Marked suppression of two enzymes, SOAT2 and GK, is assumed to play an important role in increasing lipid levels in the affected liver, bringing about hepatic steatosis.

HABP2 and SERPINE1 appear to synergistically facilitate the formation of blood clots, and these two proteins are further boosted by KNG1. It has been reported that rapid and large ingestion of ethanol predisposes us to grave thrombosis and embolism in vessels, especially in the coronary arteries (26).

The effects of suppressing these three enzymes might be part of a mechanism explaining these clinical phenomena.

The results from qPCR and western blotting indicate that ADORA1 is located further upstream than caspase 3 on the stream of signal transduction that starts with ethanol intake into the cells. The actin amount seems to correlate well with the severity of stresses. Therefore, actin is suggested as an appropriate biomarker, since it is abundant and changes are believed to have reliable sensitivity and specificity to reflect stress severity.

On the heatmap (Fig. 5A), each time point has its own cluster(s) of upregulated gene expression contrasting with other time points, so there is no uniform pattern of gene expression during the time course examined. It seems that when pathways are activated, each sub-cascade is sequentially activated. Based on this observation, it is hypothesized that overall cascade is sectioned (Fig. 5B) into a series of sub-cascades. In this hypothesis, after a substance enters a cell, a first key molecule is produced that signals for the nuclei to run a pre-determined program which activates genes governing the first section of the pathway. A first set of enzymes thus made reaches the first key molecule, leading to rapid signal transduction in the first sub-cascade. This first sub-cascade produces a second key molecule. Then, this second key molecule similarly activates the DNAs to produce the prerequisite enzymes that get delivered to implement a second sub-cascade. This yields a third key molecule. After executing each sub-cascade, final products are thought to cause observable outcomes or symptoms such as inflammation, fever, or clot formation.

Arguably the gene expression pattern (Fig. 5A), is separated into two groups. Genes upregulated in the medium only are downregulated under ethanol stimulation, whereas genes upregulated under ethanol stimulation are downregulated in the medium only. This means proteins that reacted to ethanol are primarily induced without conserved proteins. This may explain why there are time lags following ethanol ingestion before the expression of symptoms in patients suffering after binge drinking.

ADORA1-siRNA showed significant suppression of actin protein expression and ROS suppression that clearly follows ADORA1-siRNA transfection at both 3hr and 48hr. It has been reported that the apoptosis pathway consists of two distinct signal transduction streams, and that one is activated through caspases and the other through ROS generation (KEGG apoptosis pathway, URL: <https://www.genome.jp/pathway/hsa04210>). These data indicate that adenosine A1 receptors in the liver contribute to apoptosis leading to liver damage in acute alcoholism through both intrinsic pathway and reactive oxygen species activity. Animal studies should be an appropriate and practical next step to examine the magnitude of ADORA1-siRNA effects that can be elicited clinically.

In this study, physiological hepatocytes are shown to ultimately self-destruct in apoptosis, and the stresses appear to synergistically build up and accelerate the gravity of liver damage, following well-orchestrated and synergistic signal transduction pathways set in motion by an acute large bolus influx of ethanol. It is assumed that the molecules brought about by ethanol stimulation are induced proteins and not conserved proteins. It is hypothesized that each sub-cascade is executed promptly with delivery of

the set of prerequisite enzymes, and these sub-cascade processes take place in sequence.

In conclusion, the results of these experiments suggest that ADORA1 plays a significant role in ethanol-induced metabolism in hepatocytes. ADORA1 is involved in the regulation of ROS production and apoptosis. Blocking ADORA1 with siRNA can reduce the production of ROS and apoptosis in the hepatocytes cultured with ethanol. Actin is proposed to be an appropriate biomarker for evaluation of the degree of liver damage.

Acknowledgements

The authors appreciate Dr. Mothomang and Dr. Ntchobo for discussions as well as all the staff at MagBio company for their support and assistance. We also appreciate Dr. Jurgen Schnermann for providing A1R knockout mice.

Author contributions

G.H contributed to resources and project administration. T.N. contributed to investigation and writing – review & editing.

Data availability

The datasets generated and analyzed during the current study are available in the NCBI SRA repository with accession number SRX19524277.

Competing interests

The authors declare no competing interests.

Supplementary Information

This article contains Supplementary Information.

Funding

This work was supported by NT Biologics.

Abbreviations

ANOVA	analysis of variance
ARHGEF26	Rho guanine nucleotide exchange factor (GEF) 26
CDC42BPG	CDC42 binding protein kinase gamma
CEBPB	CCAAT/enhancer binding protein beta
CTGF	connective tissue growth factor
CYP2E1	cytochrome P450 family 2 subfamily E member 1
DDIT4	DNA-damage-inducible transcript 4

GAPDH	glyceraldehyde 3-phosphate dehydrogenase
GK	glycerol kinase
HABP2	hyaluronan-binding protein 2
HLA	human leukocyte antigen
HRP	horseradish peroxidase
ID1	inhibitor of DNA binding 1
IER3	immediate early response 3
IGFBP1	insulin-like growth factor binding protein 1
KNG1	kininogen-1
LYZ	lysozyme
NOXA1	NADPH oxidase activator 1
OXT	oxytocin/neurophysin I prepropeptide
PHLDA2	pleckstrin homology-like domain family A member 2
PTGDR2	prostaglandin D2 receptor 2
SERPINE1	plasminogen activator inhibitor-1
SLC2A1	solute carrier family 2, facilitated glucose transporter member 1
SOAT2	sterol O-acyltransferase 2

References

1. H. T, A. K, A.R. M. How to modulate inflammatory cytokines in liver diseases. Vol. 26, Liver International. 2006.
2. Elnagdy M, Barve S, McClain C, Gobejishvili L. cAMP signaling in pathobiology of alcohol associated liver disease. Vol. 10, Biomolecules. 2020.
<https://doi.org/10.3390/biom10101433>
3. Lee YJ, Shukla SD. Pro- and anti-apoptotic roles of c-Jun N-terminal kinase (JNK) in ethanol and acetaldehyde exposed rat hepatocytes. Eur J Pharmacol. 2005;508(1–3). <https://doi.org/10.1016/j.ejphar.2004.12.006>
4. Summary of 2012 RSA Posters/Abstracts. Alcohol Clin Exp Res. 2012;36.
<https://doi.org/10.1111/j.1530-0277.2012.01802.x>
5. Elbashir SM, Harborth J, Lendeckel W, Yalcin A, Weber K, Tuschl T. Duplexes of 21-nucleotide RNAs mediate RNA interference in cultured mammalian cells. Nature. 2001;411(6836). <https://doi.org/10.1038/35078107>
6. Fire A, Xu S, Montgomery MK, Kostas SA, Driver SE, Mello CC. Potent and specific genetic interference by double-stranded RNA in caenorhabditis elegans. Nature. 1998;391(6669). <https://doi.org/10.1038/35888>
7. Nagata T, Redman RS, Lakshman R. Isolation of intact nuclei of high purity from mouse liver. Anal Biochem. 2010;398(2). <https://doi.org/10.1016/j.ab.2009.11.017>
8. Mishra M, Tiwari S, Gunaseelan A, Li D, Hammock BD, Gomes A v. Improving the sensitivity of traditional Western blotting via Streptavidin containing Poly-horseradish peroxidase (PolyHRP). Electrophoresis. 2019;40(12–13).
<https://doi.org/10.1002/elps.201900059>
9. Choi-Miura NH, Yoda M, Saito K, Takahashi K, Tomita M. Identification of the substrates for plasma hyaluronan binding protein. Biol Pharm Bull. 2001;24(2).
10. Choi-Miura NH, Tobe T, Sumiya JI, Nakano Y, Sano Y, Mazda T, et al. Purification and characterization of a novel hyaluronan-binding protein (PHBP) from human plasma: It has three EGF, a kringle and a serine protease domain, similar to hepatocyte growth factor activator. J Biochem. 1996;119(6).
<https://doi.org/10.1093/oxfordjournals.jbchem.a021362>
11. Römisch J, Vermöhlen S, Feussner A, Stöhr HA. The FVII activating protease cleaves single-chain plasminogen activators. Haemostasis. 1999;29(5).
<https://doi.org/10.1159/000022515>

12. Benezra R, Davis RL, Lockshon D, Turner DL, Weintraub H. The protein Id: A negative regulator of helix-loop-helix DNA binding proteins. *Cell*. 1990;61(1). [https://doi.org/10.1016/0092-8674\(90\)90214-Y](https://doi.org/10.1016/0092-8674(90)90214-Y)
13. Ellisen LW, Ramsayer KD, Johannessen CM, Yang A, Beppu H, Minda K, et al. REDD1, a developmentally regulated transcriptional target of p63 and p53, links p63 to regulation of reactive oxygen species. *Mol Cell*. 2002;10(5). [https://doi.org/10.1016/S1097-2765\(02\)00706-2](https://doi.org/10.1016/S1097-2765(02)00706-2)
14. Luo D, Jin B, Zhai X, Li J, Liu C, Guo W, et al. Oxytocin promotes hepatic regeneration in elderly mice. *iScience*. 2021;24(2). <https://doi.org/10.1016/j.isci.2021.102125>
15. Geddes R, Straton GC. The influence of lysosomes on glycogen metabolism. *Biochemical Journal*. 1977;163(2). <https://doi.org/10.1042/bj1630193>
16. Nitulescu GM, van de Venter M, Nitulescu G, Ungurianu A, Juzenas P, Peng Q, et al. The Akt pathway in oncology therapy and beyond (Review). Vol. 53, *International Journal of Oncology*. 2018. <https://doi.org/10.3892/ijo.2018.4597>
17. Ehrlich HJ, Klein Gebbink R, Keijer J, Linders M, Preissner KT, Pannekoek H. Alteration of serpin specificity by a protein cofactor. Vitronectin endows plasminogen activator inhibitor 1 with thrombin inhibitory properties. *Journal of Biological Chemistry*. 1990;265(22). [https://doi.org/10.1016/s0021-9258\(19\)38262-6](https://doi.org/10.1016/s0021-9258(19)38262-6)
18. Tunster SJ, Creeth HDJ, John RM. The imprinted Phlda2 gene modulates a major endocrine compartment of the placenta to regulate placental demands for maternal resources. *Dev Biol*. 2016;409(1). <https://doi.org/10.1016/j.ydbio.2015.10.015>
19. Pramfalk C, Angelin B, Eriksson M, Parini P. Cholesterol regulates ACAT2 gene expression and enzyme activity in human hepatoma cells. *Biochem Biophys Res Commun*. 2007;364(2). <https://doi.org/10.1016/j.bbrc.2007.10.028>
20. Garcia J, Ye Y, Arranz V, Letourneux C, Pezeron G, Porteu F. IEX-1: A new ERK substrate involved in both ERK survival activity and ERK activation. *EMBO Journal*. 2002;21(19). <https://doi.org/10.1093/emboj/cdf488>
21. Hamidi T, Algül H, Cano CE, Sandi MJ, Molejon MI, Riemann M, et al. Nuclear protein 1 promotes pancreatic cancer development and protects cells from stress by inhibiting apoptosis. *Journal of Clinical Investigation*. 2012;122(6). <https://doi.org/10.1172/JCI60144>
22. Letourneux C, Rocher G, Porteu F. B56-containing PP2A dephosphorylate ERK and their activity is controlled by the early gene IEX-1 and ERK. *EMBO Journal*. 2006;25(4). <https://doi.org/10.1038/sj.emboj.7600980>

23. Lieber CS. Microsomal ethanol-oxidizing system (MEOS): The first 30 years (1968- 1998) - A review. Vol. 23, Alcoholism: Clinical and Experimental Research. 1999. <https://doi.org/10.1111/j.1530-0277.1999.tb04217.x>
24. Huot J, Houle F, Rousseau S, Deschesnes RG, Shah GM, Landry J. SAPK2/p38-dependent F-actin reorganization regulates early membrane blebbing during stress-induced apoptosis. *Journal of Cell Biology*. 1998;143(5). <https://doi.org/10.1083/jcb.143.5.1361>
25. Osna NA, Donohue TM, Kharbanda KK. Alcoholic Liver Disease: Pathogenesis and Current Management. Vol. 38, Alcohol research : current reviews. 2017.
26. van de Wiel A, van Golde PM, Kraaijenhagen RJ, von dem Borne PAK, Bouma BN, Hart HC. Acute inhibitory effect of alcohol on fibrinolysis. *Eur J Clin Invest*. 2001;31(2). <https://doi.org/10.1046/j.1365-2362.2001.00773>.

Figure legends

Figure 1: Chronological changes of ADORA1, caspase3 full-length, and GAPDH using quantitative real time PCR (qPCR). Hepatocytes were cultured for 0 (control), 1.5, 3 or 6 hours after the addition of ethanol at 100mM.

- (A) ADORA1 gene expression. X-axis shows the time after adding ethanol into the culture medium at 100mM. Values represent the mean and the standard error of mean (SEM). T-Test, *: $p = 0.0048$
- (B) Gene expression of caspase3 full-length. X-axis shows the time after adding ethanol into the culture medium at 100mM. Values represent the mean and the standard error of mean (SEM). T-Test, **: $p = 0.0047$
- (C) Gene expression of GAPDH as a housekeeping gene. X-axis shows the time after adding ethanol into the culture medium at 100mM. Values represent the mean and the standard error of mean (SEM). No significance was seen among three time points.

Figure 2: Western blot analysis of ADORA1, actin, GAPDH, and caspase 3 was performed on hepatocytes cultured for 48 hours with and without 100mM ethanol (EtOH). Each sample was normalized to GAPDH. Alternatively, normalization with total loaded amount of protein was also performed (Figure S2). Poly-HRP conjugated secondary antibodies were used to enhance signals (Mishra et al., 2019). Lane 1: Cells cultured in medium only. Lane 2: Cells cultured with 100mM ethanol. Lane 3: Cells cultured with 100mM ethanol. Lane 4: Cells cultured in medium only. Lane 5: Cells cultured with 100mM ethanol.

- (A) The expressions of ADORA1 and actin were measured in medium with and without 100mM ethanol. No signals were detected for ADORA1 in medium only. The images are shown above and their quantified data is shown below. T-test analysis demonstrated that the both expressions of ADORA1 and actin were notably increased in the presence of ethanol ($*p = 0.04$; $**p = 0.02$).
- (B) The expression levels of caspase 3 were also measured in medium with and without 100mM ethanol. The images are shown above, and the quantified data is shown below. The expression levels of caspase 3 were significantly increased in the presence of ethanol.

Figure 3: The analysis of signal transduction mechanisms and kinetics with Next Generation Sequencing. Samples were taken at 0 (control), 1.5, 3 and 6hr in the time course of cultures in the medium with 100mM of ethanol. NovoSmart (Novogene), Cytoscape, UniProt, and KEGG PATHWAY Database were employed for the analysis. In (B) through (D), functional enrichments in the network of protein-coding genes through the time course are shown.

- (A) Heatmap comparison of gene expression at all four time points. A list of

expressed gene symbols and names is available in Supporting information Figure S2.

- (B) Gene interactions and comparisons between 0 and 1.5hr. The width of each line is proportional to the strength of interaction between each neighbor. Circle sizes express the difference in expression intensity, where the size of the circles is proportional to the ratio ($\log_2\text{Fold}$) of the expression level at 1.5hr to that at 0hr. The color and intensity of each circle reflects the sign and magnitude of the values ($\log_2\text{Fold}$), where blue means it is negative and red is positive.
 $-7.68 < \log_2\text{Fold} < 7.88$.
- (C) Gene interactions and comparisons between 0 and 3hr. Circles express the difference in expression intensity, where the size of the circles reflects the ratio ($\log_2\text{Fold}$) of the expression level at 3hr to that at 0hr. The color and intensity of each circle reflects the sign and magnitude of the values ($\log_2\text{Fold}$), where blue means it is negative and red is positive.
 $-7.05 < \log_2\text{Fold} < 7.79$.
- (D) Gene interactions and comparisons between 0 and 6hr. Circles express the difference in expression intensity, where the size of the circles reflects the ratio ($\log_2\text{Fold}$) of the expression level at 6hr to that at 0hr. The color and intensity of each circle reflects the sign and magnitude of the values ($\log_2\text{Fold}$), where blue means it is negative and red is positive.
 $-3.58 < \log_2\text{Fold} < 7.74$.

Figure 4: Evaluation of ADORA1-siRNA transfection into hepatocytes.

Hepatocytes were transfected with ADORA1-siRNA followed by culture in medium containing 100mM of ethanol. This figure presents the results of western blot analysis (A), reactive oxygen species (ROS) assay (B), and morphological evaluation (C).

- (A) Hepatocytes transfected with ADORA1-siRNA were then cultured for 48 hours in 100mM ethanol (EtOH) along with the cells cultured in medium only and the cells cultured only in 100mM ethanol (EtOH). Each sample was normalized to GAPDH of the same group. Poly-HRP conjugated secondary antibodies were used to enhance signals. Actin expression cultured with 100mM ethanol notably decreased with the transfection of ADORA1-siRNA into the hepatocytes. T-test: $*p = 0.007$.
- (B) Reactive Oxygen Species (ROS) assay with ADORA1-siRNA. The hepatocytes were cultured for 3 or 48 hours at 100mM of ethanol with or without the transfection of ADORA1-siRNA into the hepatocytes. Antimycin A was used as the positive control and N-acetyl cysteine as the negative control. The fluorescence was measured using exciting wave length of 485nm and emission wave length of 590nm by SPECTRAMAX GEMINIEM (Molecular Devices). Data was analyzed with SoftMax Pro Software (Molecular Devices). Y-axis shows absorbances where the scale was determined by the positive and negative controls. The production of ROS was significantly increased at 48

hours compared to 3 hours in the hepatocytes cultured with 100mM ethanol (* $p = 0.02$). The production of ROS was significantly decreased in the hepatocytes cultured with 100mM ethanol and the transfection of ADORA1-siRNA at both 3 hours and 48 hours (** $p = 0.04$).

- (C) Phase-contrast microscopy was used to visualize the morphology of hepatocytes cultured for 46 hours with medium only, 100mM ethanol, or 100mM ethanol and ADORA1-siRNA. Apoptotic bodies and lipid droplets were observed in the hepatocytes cultured with 100mM ethanol (b). The number of apoptotic bodies and lipid droplets was significantly decreased in the hepatocytes cultured with 100mM ethanol and ADORA1-siRNA (c). No such abnormalities were observed in the hepatocytes cultured with medium only (a).

Figure 5: A hypothesis for the system of ethanol induced signal transduction.

This figure shows a hypothesis for the system of ethanol-induced signal transduction. The hypothesis is based on the results of NGS data analysis (A) and a diagram (B).

- (A) Heatmap obtained from analysis of NGS data on gene expression in hepatocytes cultured in medium with 100mM of ethanol (identical to Fig. 3A): The areas framed in black are upregulated clusters associated with specific time points. One asterisk indicates the control group where the hepatocytes were cultured only in medium. Two asterisks indicate the group where the hepatocytes were cultured in 100mM of ethanol for 1.5 hours. Three asterisks represent the group where the hepatocytes were cultured in 100mM of ethanol for 3 hours. Four asterisks represent the group where the hepatocytes were cultured in 100mM of ethanol for 6 hours.
- (B) The diagram illustrates the hypothesis: (1) Substrate (ethanol in this case) enters the cell through its receptors (CYP2E1 in this case) and undergoes first reactions in the pathway. (2) A first key molecule is produced and sends a signal to run the first program in the nuclei. (3) The initial set of enzymes is produced by the program. (4) This first set of enzymes is delivered to the first key molecule. (5) The reactions of the first sub-cascade are executed. (6) A second key molecule is produced and sends a signal to run a second program in the nuclei. (7) A second set of enzymes is produced by the program. (8) The second set of enzymes is delivered to the second key molecule. (9) The reactions in a second sub-cascade are executed. (10) A third key molecule is produced and analogous cycles are repeated until the end products are produced.

Table 1**Catalogue of major genes/proteins expressed in response to ethanol stimulation.**

Gene Name	Function	Regulation	Assumed outcome
CDC42BPG ¹	Actin related	Up-regulation	Actin formation
ARHGEF26 ¹	Actin related	Up-regulation	Actin formation
ID1 ^{3*}	Actin related	Up-regulation	Actin assembly
OXT ²	Inflammation related	Up-regulation	Upregulating prostaglandin secretion
PTGDR2 ²	Inflammation related	Up-regulation	Facilitating inflammation responses
KNG1 ^{2*}	Inflammation related	Up-regulation	Release of prostaglandins
SERPINE1 ^{2*}	Inflammation related	Down-regulation	Stimulating inflammation
CEBPB ^{2*}	Inflammation related	Down-regulation	Aggression of acute-phase reaction
ID1 ^{3*}	Apoptosis	Up-regulation	Upregulating apoptosis
DDIT4 ³	Inhibition of the activity of the mammalian target of rapamycin complex 1 (mTORC1).	Up-regulation	p53/TP53-mediated apoptosis
IER3 ³	ERK1/2 activation	Down-regulation	Facilitating apoptosis
CTGF ³	Activation of ERK1/2 and JNK	Down-regulation	Facilitating apoptosis
IGFBP1 ^{3*}	Activation of AKT signaling pathway	Down-regulation	Facilitating apoptosis
HABP2 ⁷	coagulation factor VII-activating	Up-regulation	Forming blood clots
KNG1 ^{7*}	blood coagulation	Up-regulation	Forming blood clots
SERPINE1 ^{7*}	thrombin inhibitor	Down-regulation	Forming blood clots
SLC2A1 ⁴	glucose uptake	Down-regulation	Reducing glucose uptake
LYZ ⁴	Glycogen release from lysosomes, becoming a final energy source	Down-regulation	No purge of glycogen, worsening Starvation state
IGFBP1 ^{4*}	glucose uptake	Down-regulation	Suppressing glucose uptake
CEBPB ^{4*}	Gluconeogenesis	Down-regulation	Down-regulation of gluconeogenesis
PHLDA2 ⁴	Controlling glycogen storage	Down-regulation	Down-regulation of glycogenolysis
SOAT2 ⁵	Secretion of cholesteryl esters	Down-regulation	Retaining of lipids in the cells
GK ⁵	Controlling glycerol uptake	Down-regulation	facilitating steatosis
NOXA1 ⁶	NADPH oxidase producing superoxide	Up-regulation	inducing ROS production

*: Molecules having more than one function have repeat entries for each function.

Superscript codes for each functional group are as follows:

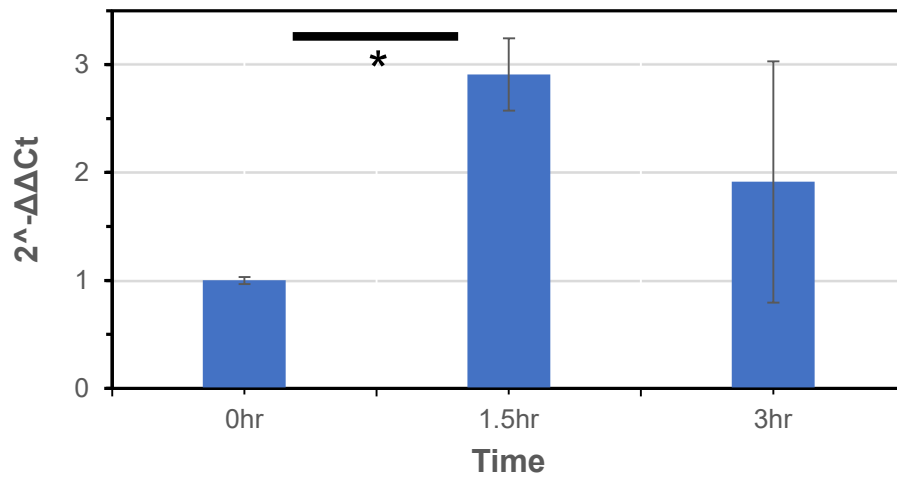
1: actin formation related; 2: inflammation related; 3: apoptosis related; 4: Energy related; 5: Steatosis related; 6: ROS related; 7: blood coagulation related.

Table 2
The sequences of primer pairs

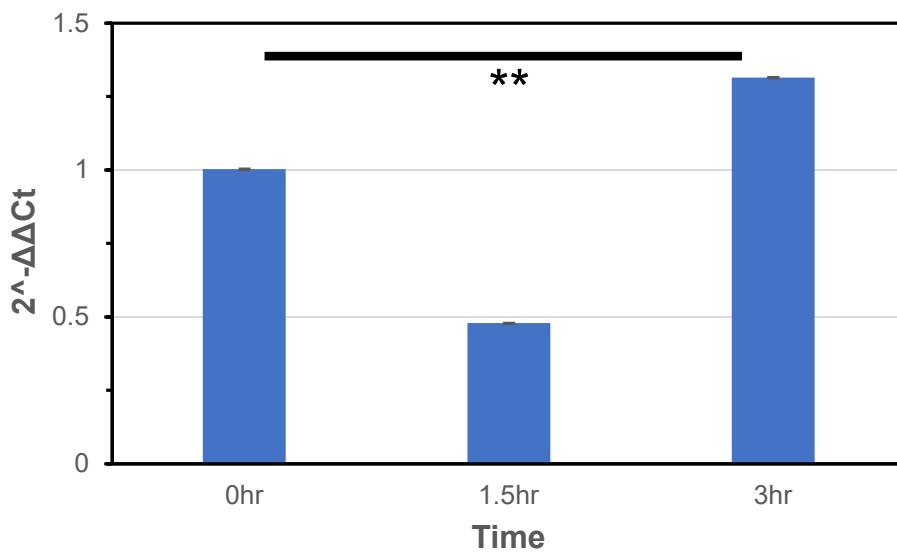
Gene	Forward (5' – 3')	Length (bp)	Reverse (5' – 3')	Length (bp)
ADORA1	CCTCCATCTCAGCT TTCCAG	20	AGTAGGTCTGTGG CCCAATG	20
Caspase 3 full length	GGCACAAAGCGAC TGGAT	18	TGGCACAAAGCGA CTGGAT	19
Casp-3p17	TGGAATTGATGCGT GATGTT	20	GGCAGGCCTGAA TAATGAAA	20
GAPDH	CCCTGGCCAAGGT CATCC	18	TGATGGCATGGAC TGTGGTC	20

Figure 1

A



B



C

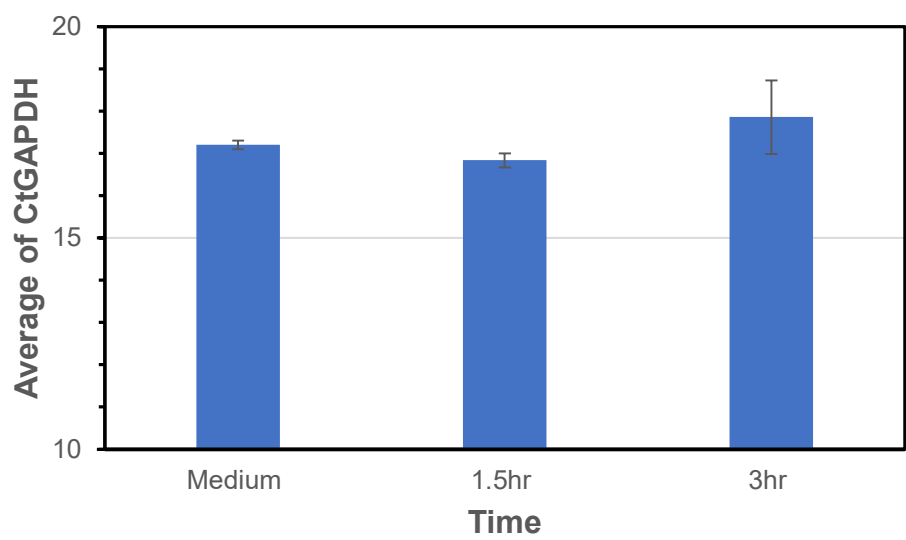
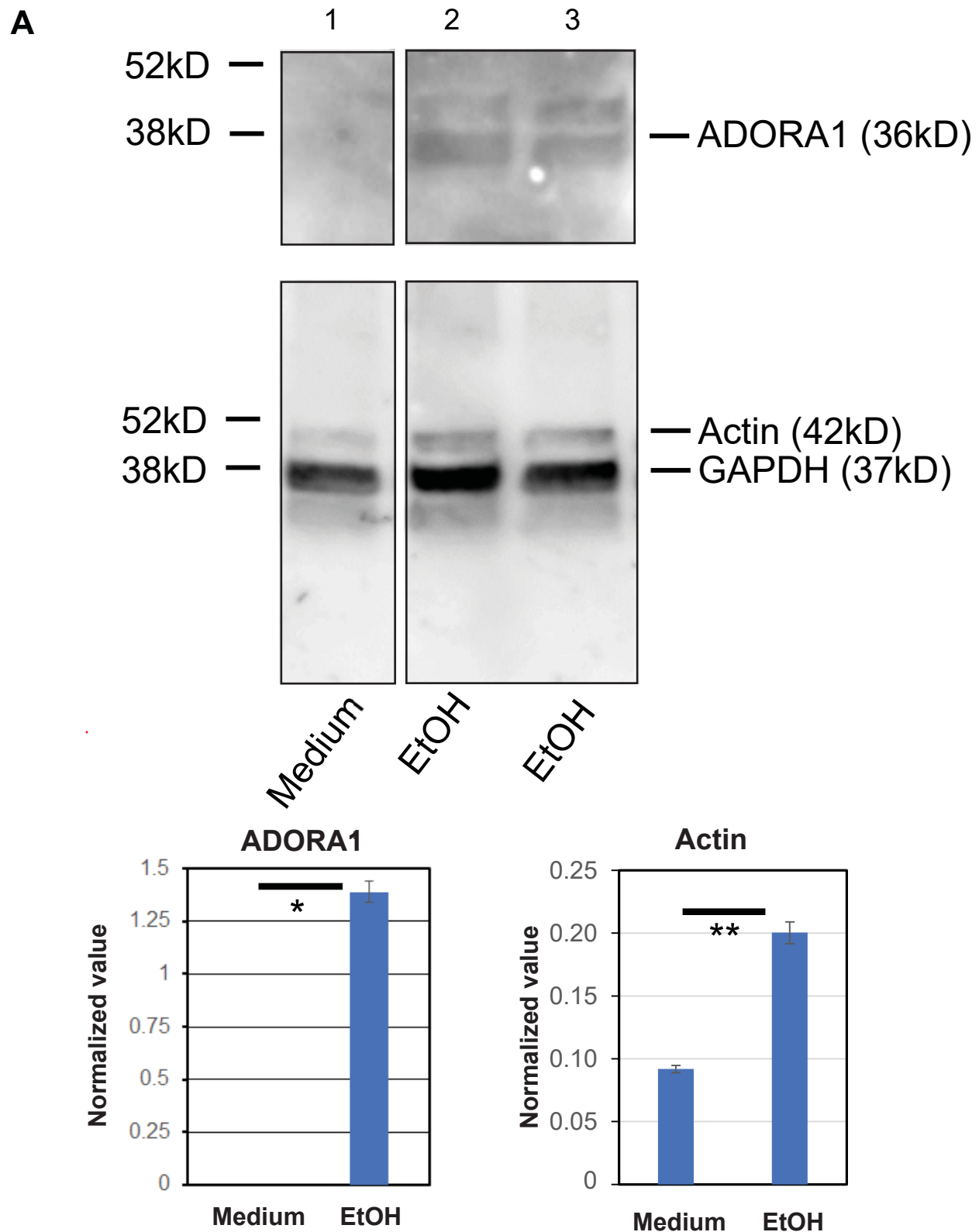


Figure 2



B

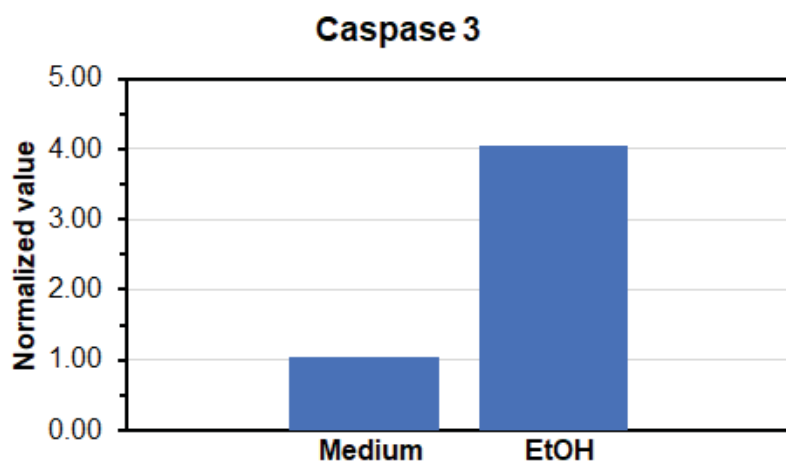
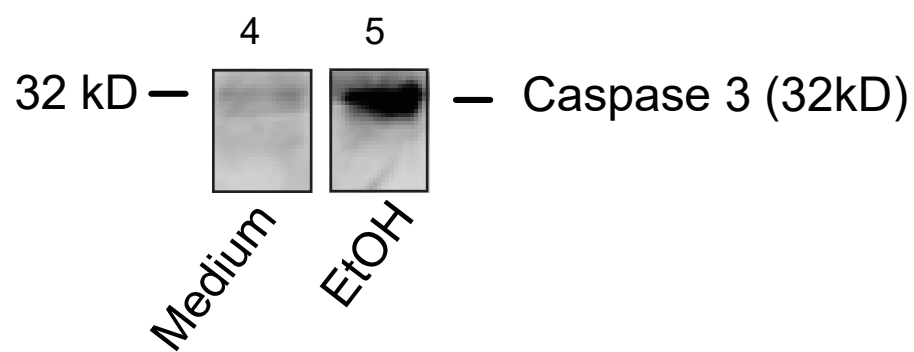
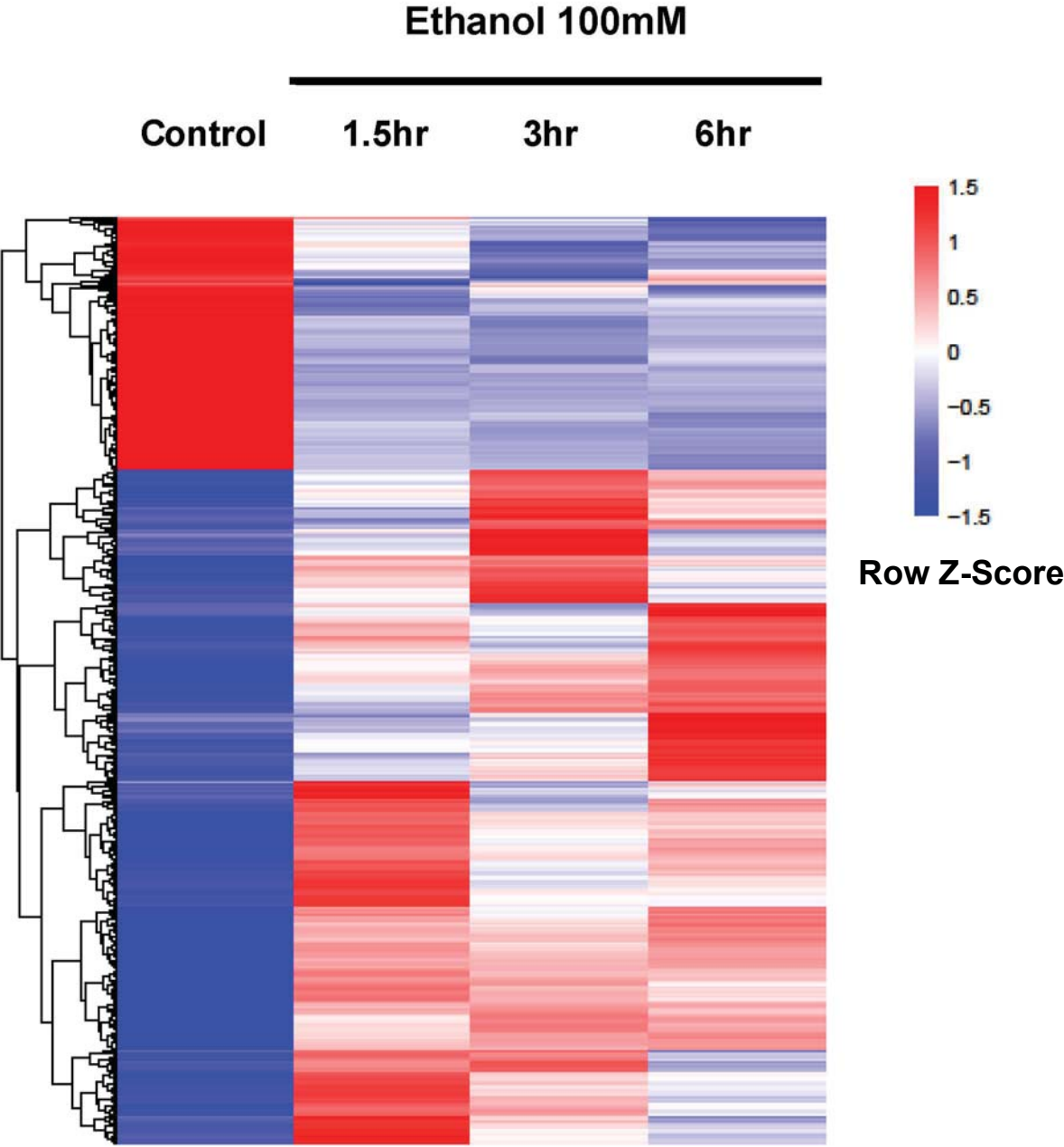


Figure 3

A



[illegible]

D

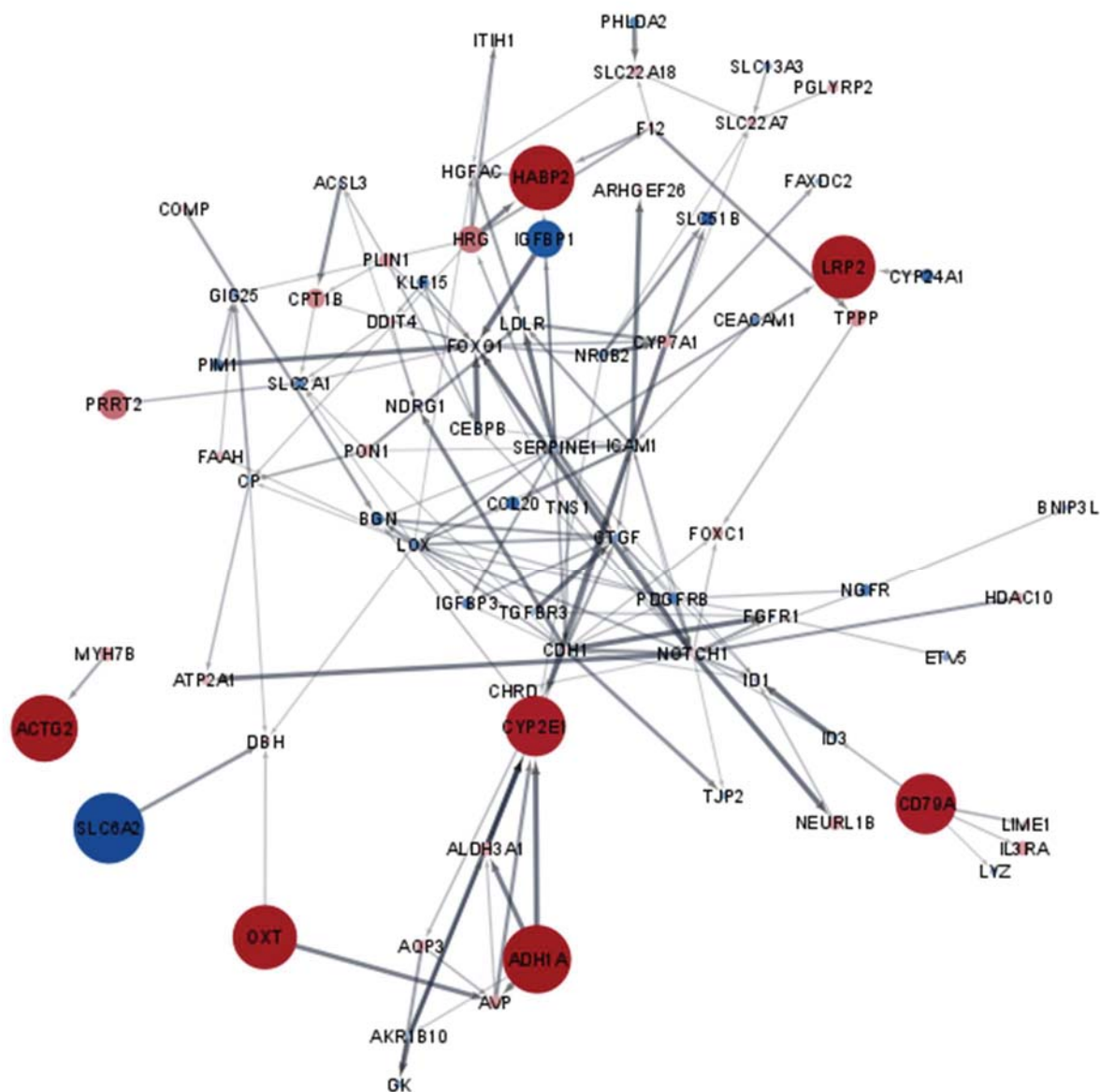
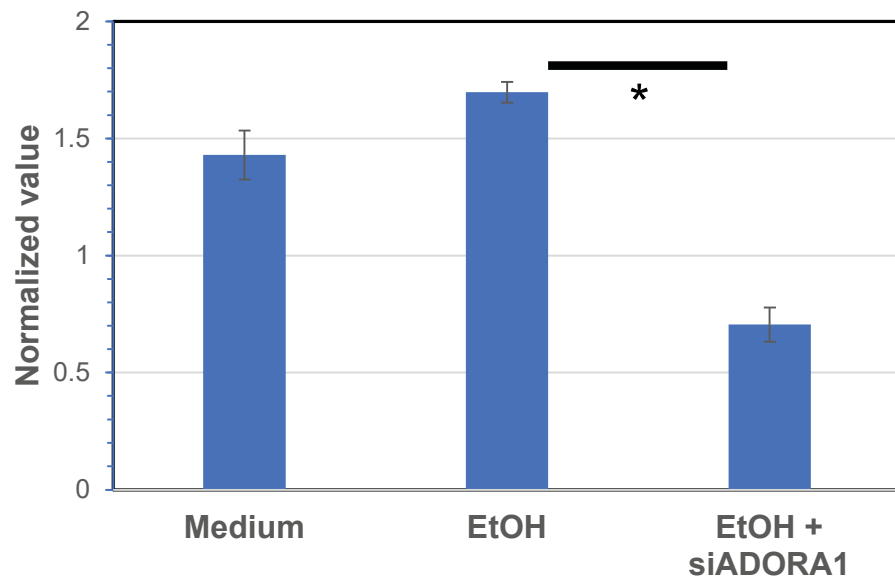
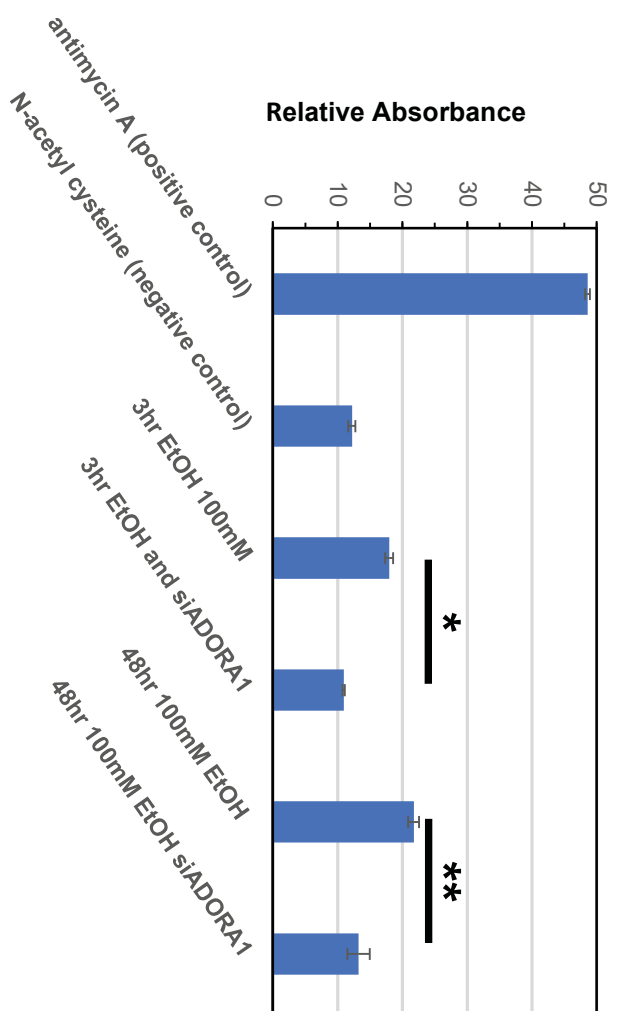


Figure 4

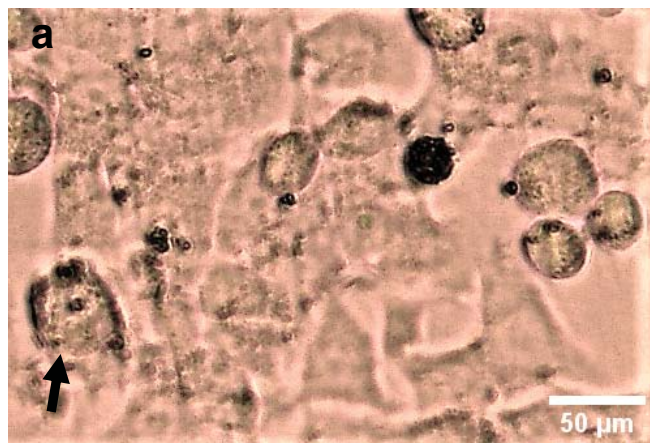
A



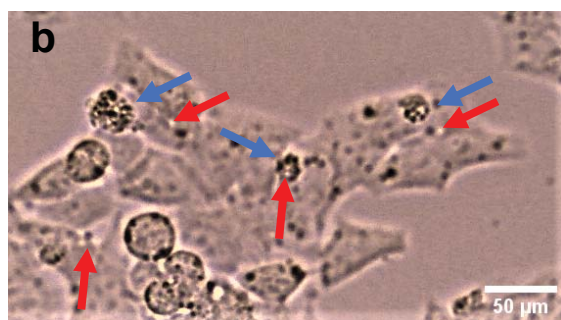
B



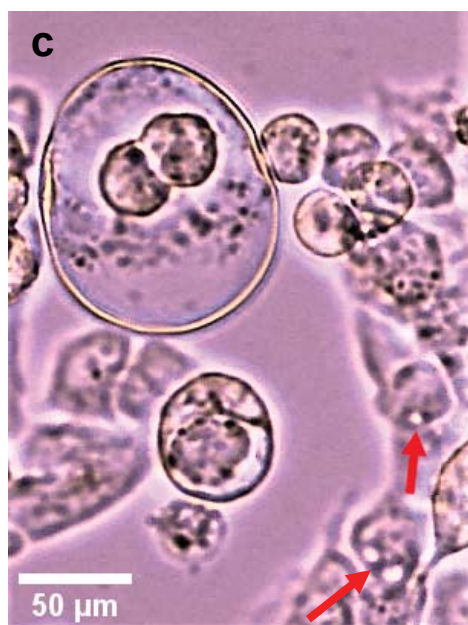
C



Hepatocytes in medium only



Hepatocytes in 100mM of ethanol



Hepatocytes in 100mM of ethanol with ADORA1-siRNA




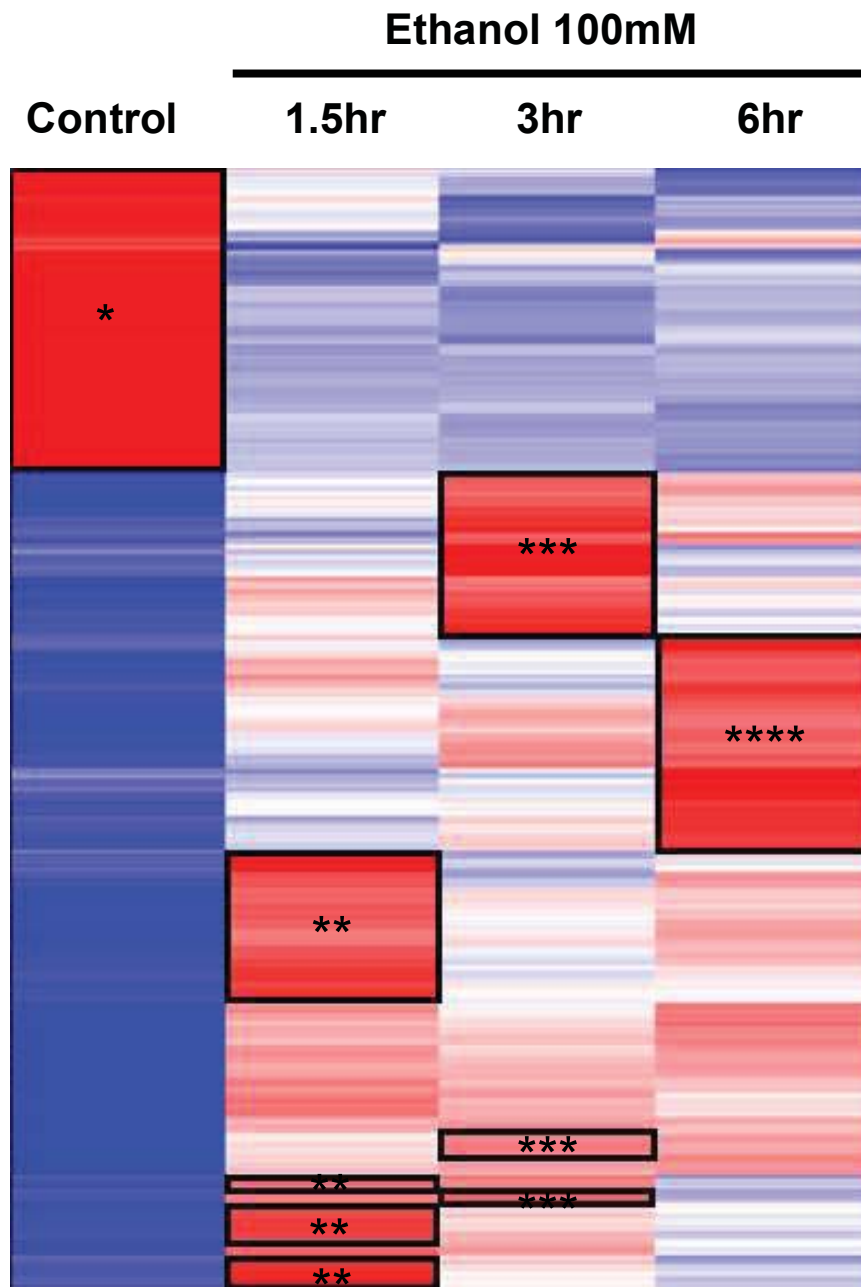
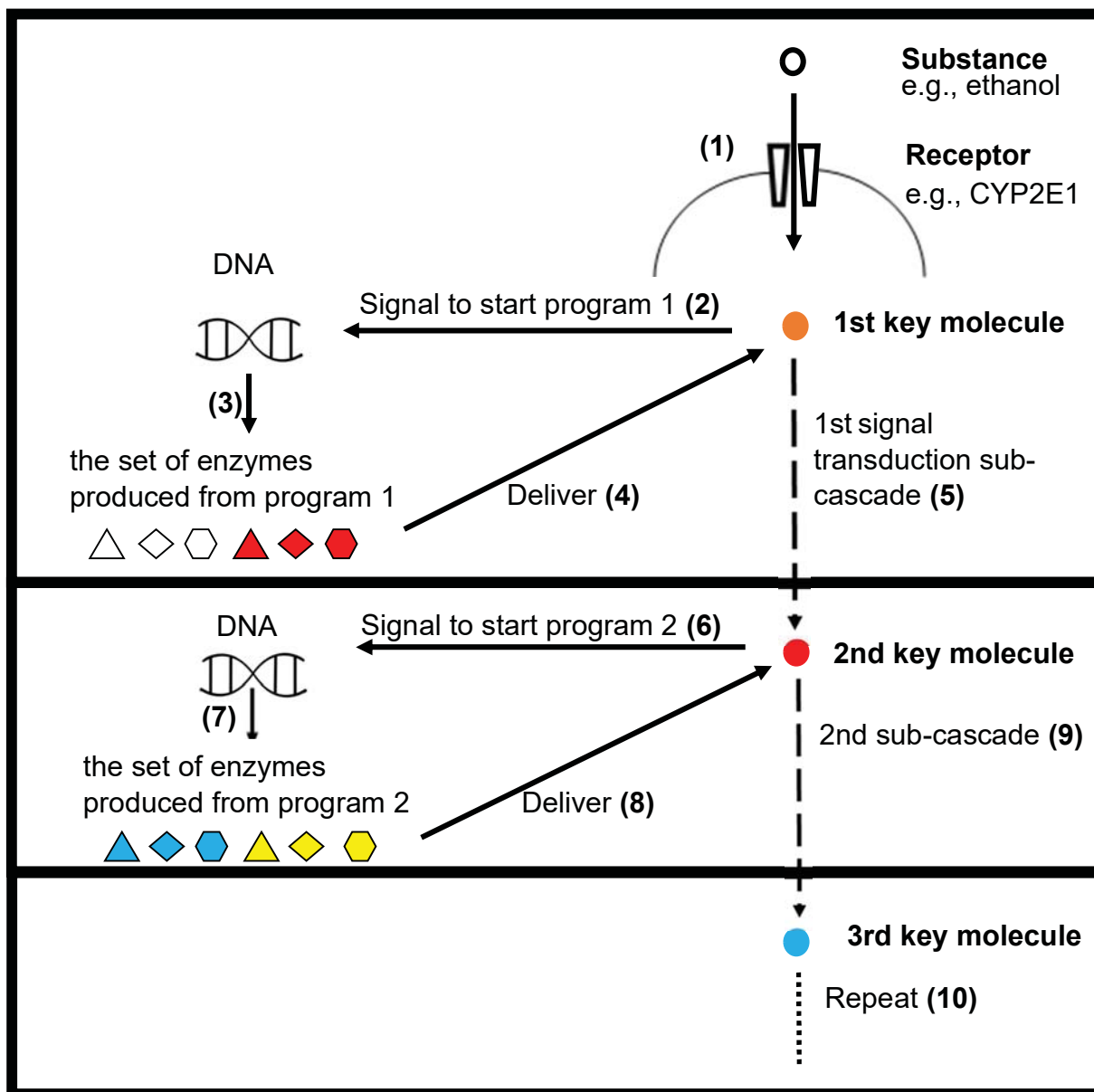
- | | |
|---|-----------------------------|
|  | normal nucleus |
|  | apoptotic bodies |
|  | lipid droplets (white dots) |

Figure 5

A



B



Supplementary Material

Elucidating the role of intrinsic adenosine A1 receptors in acute alcoholism using human induced pluripotent stem cell-derived hepatocytes

Takako Nagata, Yuning George Huang

List of material included:

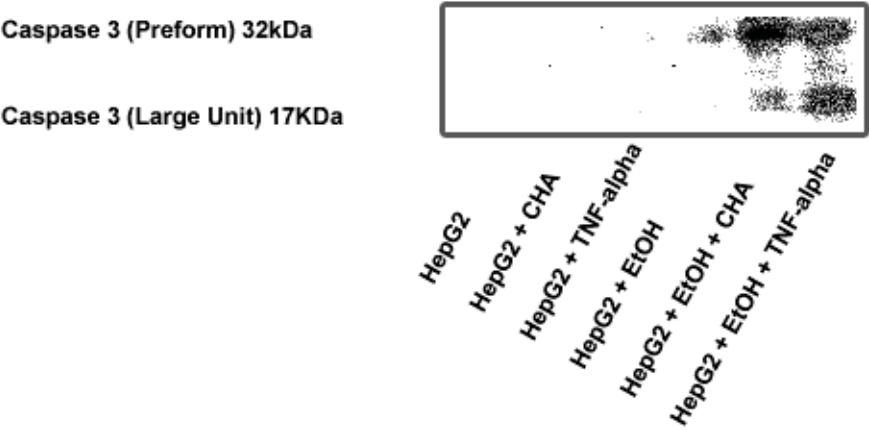
Figure S1: Role of adenosine A1 receptors in exacerbation of inflammation and liver damage under excessive alcohol consumption

Figure S2: Western blot analysis of ADORA1 and actin (supplement data for Figure 2A)

Table S1: List of expressed gene symbols and names in the order they appear on the heatmap in Figure 3A

Figure S1

A



B

TNF- α (pg/ml)		
Wildtype	92.5 \pm 10.6	
A1R KO	11.9 \pm 5.9	

Figure S1: Role of adenosine A1 receptors in exacerbation of inflammation and liver damage under excessive alcohol consumption.

In vivo, adenosine A1 receptor knockout mice (A1R KO) with C57BL/6 background (8wk old, male, 25g), and wild-type from the same colonies were employed. N6-cyclohexyladenosine (CHA), A1 agonist, from Tocris, was intraperitoneally injected at 0.3 mg/kg. At 30 min, ethanol (EtOH) was intraperitoneally injected at 3.6 g/kg. Sera at 1.5 hours were assayed for TNF- α as an inflammation level indicator. In vitro, HepG2 (liver hepatocellular carcinoma) cell line at 3×10^5 cells / ml / well, was cultured with ethanol at 100mM or with EtOH at 100mM and CHA at 10^{-5} M. TNF- α (1ng/ml) was used to make the positive controls. The cells were harvested after 45-hour culture to assess TNF- α and caspase 3 (preform and the large unit of activated form) using western blotting. Caspase 3 was detected with anti-caspase 3 antibody from Santa-Cruz Biotechnology. Total protein was measured with Protein Assay from Bio-Rad. 10ug of protein was loaded in each lane.

- (A) Caspase 3 expression in HepG2 with EtOH and CHA: Co-stimulation of EtOH and CHA caused significantly higher expression of preform caspase 3 which was even higher than the positive control with EtOH and TNF- α , while EtOH stimulation alone caused mild increase in preform caspase 3. Activated caspase 3 was also induced by co-stimulation of EtOH and CHA, while no such induction was observed with EtOH alone. Total protein yielded from cultures with EtOH + CHA and with EtOH + TNF- α at 45 hr was below 65 % of that from HepG2 alone. TNF- α was not detected in the samples from HepG2 alone, HepG2 + CHA, HepG2 + EtOH, or HepG2 + EtOH + CHA).
- (B) TNF- α with EtOH in C57BL/6 mice & A1R KO: At 1.5 hours after ethanol injection, TNF- α values were markedly higher in the wild type group than in the A1R KO group (n = 5 to 6 per group).

Figure S2

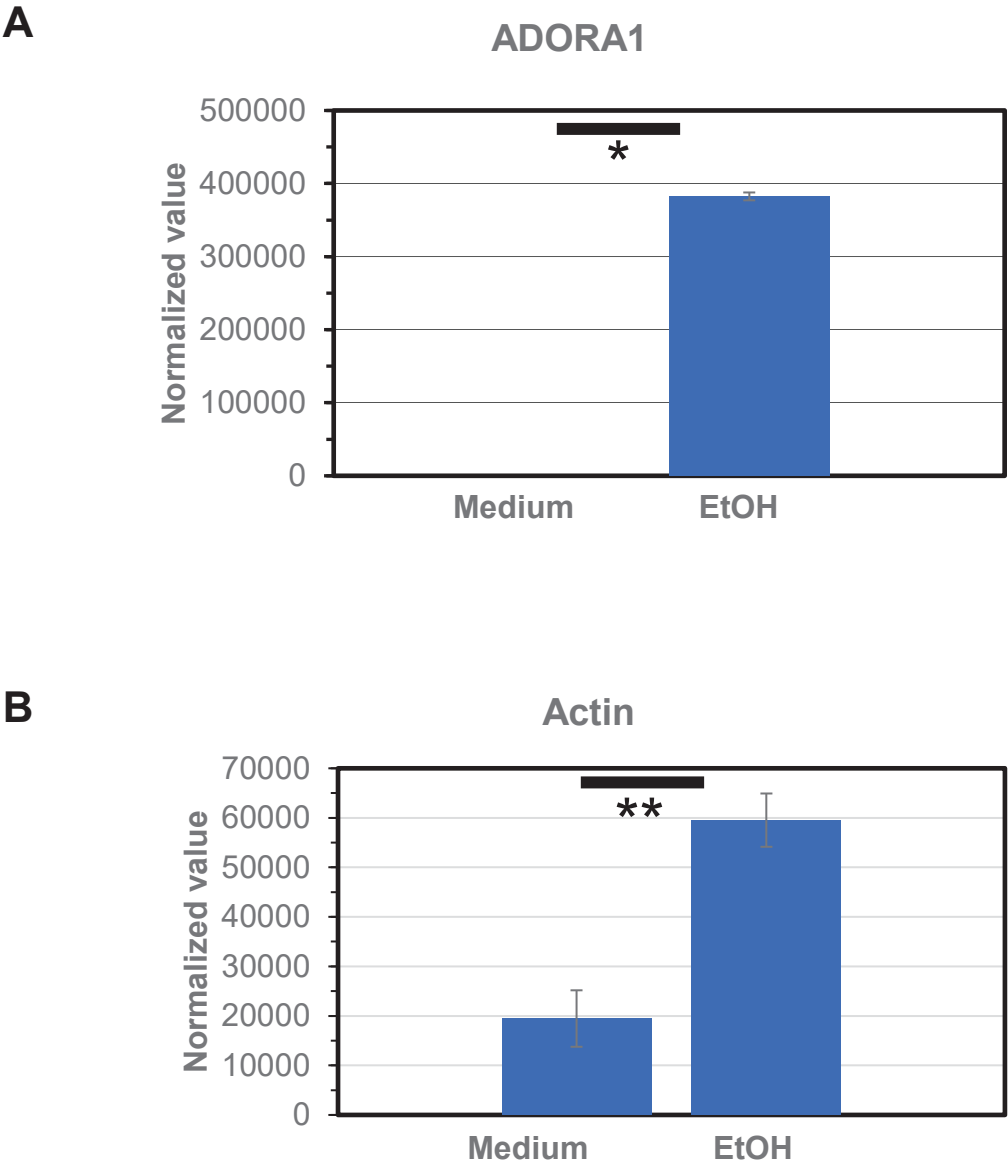


Figure S2: Western blot analysis of ADORA1 and actin (supplement data for Figure 2A). Each measured volume of signals for ADORA1 and actin was respectively normalized to the amount of total loaded protein. Both ADORA1 and actin demonstrated equivalent results to Figure 2A.

- (A) ADORA1 protein expression was normalized to its total loaded amount (μg). T-test analysis showed that ADORA1 protein expression was remarkably increased in the presence of ethanol (* $p=0.004$).
- (B) Actin protein expression was normalized to its total loaded amount (μg). T-test analysis showed that actin protein expression was significantly increased in the presence of ethanol (** $p=0.04$).

Table S1: List of expressed gene symbols and names in the order they appear on the heatmap in Figure 3A (Excel file).

ENSEMBL	SYMBOL	GENENAME
ENSG00000118523	CCN2	cellular communication network factor 2
ENSG00000137193	PIM1	Pim-1 proto-oncogene, serine/threonine kinase
ENSG00000084110	HAL	histidine ammonia-lyase
ENSG00000186198	SLC51B	solute carrier family 51 beta subunit
ENSG00000163884	KLF15	Kruppel like factor 15
ENSG00000059804	SLC2A3	solute carrier family 2 member 3
ENSG00000165507	DEPP1	DEPP1 autophagy regulator
ENSG00000136286	MYO1G	myosin IG
ENSG00000206190	ATP10A	ATPase phospholipid transporting 10A (putative)
ENSG00000064300	NGFR	nerve growth factor receptor
ENSG00000131746	TNS4	tensin 4
ENSG00000113721	PDGFRB	platelet derived growth factor receptor beta
ENSG00000266709	MGC12916	uncharacterized protein MGC12916
ENSG00000146674	IGFBP3	insulin like growth factor binding protein 3
ENSG00000198814	GK	glycerol kinase
ENSG00000185262	UBALD2	UBA like domain containing 2
ENSG00000106003	LFNG	LFNG O-fucosylpeptide 3-beta-N-acetylglucosaminyltrans
ENSG00000169604	ANTXR1	ANTXR cell adhesion molecule 1
ENSG00000019186	CYP24A1	cytochrome P450 family 24 subfamily A member 1
ENSG00000127663	KDM4B	lysine demethylase 4B
ENSG00000234199	LINC01191	long intergenic non-protein coding RNA 1191
ENSG00000088992	TESC	tescalcin
ENSG00000177984	LCN15	lipocalin 15
ENSG00000006016	CRLF1	cytokine receptor like factor 1
ENSG00000249853	HS3ST5	heparan sulfate-glucosamine 3-sulfotransferase 5
ENSG00000158296	SLC13A3	solute carrier family 13 member 3
ENSG00000101162	TUBB1	tubulin beta 1 class VI
ENSG00000115009	CCL20	C-C motif chemokine ligand 20
ENSG00000117394	SLC2A1	solute carrier family 2 member 1
ENSG00000175832	ETV4	ETS variant 4
ENSG00000110777	POU2AF1	POU class 2 homeobox associating factor 1
ENSG00000090382	LYZ	lysozyme
ENSG00000176907	TCIM	transcriptional and immune response regulator
ENSG00000074211	PPP2R2C	protein phosphatase 2 regulatory subunit Bgamma
ENSG00000236279	CLEC2L	C-type lectin domain family 2 member L
ENSG00000164683	HEY1	hes related family bHLH transcription factor with YRPW n
ENSG00000113083	LOX	lysyl oxidase
ENSG00000244405	ETV5	ETS variant 5
ENSG00000128645	HOXD1	homeobox D1
ENSG00000268104	SLC6A14	solute carrier family 6 member 14
ENSG00000160963	COL26A1	collagen type XXVI alpha 1 chain
ENSG00000079385	CEACAM1	carcinoembryonic antigen related cell adhesion molecule
ENSG00000103187	COTL1	coactosin like F-actin binding protein 1
ENSG00000103546	SLC6A2	solute carrier family 6 member 2
ENSG00000135917	SLC19A3	solute carrier family 19 member 3
ENSG00000224189	HAGLR	HOXD antisense growth-associated long non-coding RNA
ENSG00000114698	PLSCR4	phospholipid scramblase 4

ENSG00000139679	LPAR6	lysophosphatidic acid receptor 6
ENSG00000114268	PFKFB4	6-phosphofructo-2-kinase/fructose-2,6-biphosphatase 4
ENSG00000151012	SLC7A11	solute carrier family 7 member 11
ENSG00000162998	FRZB	frizzled related protein
ENSG00000159399	HK2	hexokinase 2
ENSG00000106366	SERPINE1	serpin family E member 1
ENSG00000185338	SOCS1	suppressor of cytokine signaling 1
ENSG00000061656	SPAG4	sperm associated antigen 4
ENSG00000146678	IGFBP1	insulin like growth factor binding protein 1
ENSG00000168386	FILIP1L	filamin A interacting protein 1 like
ENSG00000131910	NR0B2	nuclear receptor subfamily 0 group B member 2
ENSG00000104419	NDRG1	N-myc downstream regulated 1
ENSG00000072422	RHOBTB1	Rho related BTB domain containing 1
ENSG00000196296	ATP2A1	ATPase sarcoplasmic/endoplasmic reticulum Ca2+ transp
ENSG00000215440	NPEPL1	aminopeptidase like 1
ENSG00000117480	FAAH	fatty acid amide hydrolase
ENSG00000175265	GOLGA8A	golgin A8 family member A
ENSG00000006025	OSBPL7	oxysterol binding protein like 7
ENSG00000160781	PAQR6	progesterone and adipoQ receptor family member 6
ENSG00000266714	MYO15B	myosin XVb
ENSG00000223756	TSSC2	tumor suppressing subtransferable candidate 2 pseudoge
ENSG00000114270	COL7A1	collagen type VII alpha 1 chain
ENSG00000090539	CHRD	chordin
ENSG00000169750	RAC3	Rac family small GTPase 3
ENSG00000225756	DBH-AS1	DBH antisense RNA 1
ENSG00000188818	ZDHHC11	zinc finger DHHC-type containing 11
ENSG00000123454	DBH	dopamine beta-hydroxylase
ENSG00000254995	STX16-NPEPL1	STX16-NPEPL1 readthrough (NMD candidate)
ENSG00000145536	ADAMTS16	ADAM metalloproteinase with thrombospondin type 1 mc
ENSG00000250067	YJEFN3	YjeF N-terminal domain containing 3
ENSG00000213903	LTB4R	leukotriene B4 receptor
ENSG00000146094	DOK3	docking protein 3
ENSG00000159618	ADGRG5	adhesion G protein-coupled receptor G5
ENSG00000169026	SLC49A3	solute carrier family 49 member 3
ENSG00000187758	ADH1A	alcohol dehydrogenase 1A (class I), alpha polypeptide
ENSG00000131187	F12	coagulation factor XII
ENSG00000109758	HGFAC	HGF activator
ENSG00000197599	CCDC154	coiled-coil domain containing 154
ENSG00000054598	FOXC1	forkhead box C1
ENSG00000184925	LCN12	lipocalin 12
ENSG00000130649	CYP2E1	cytochrome P450 family 2 subfamily E member 1
ENSG00000148702	HABP2	hyaluronan binding protein 2
ENSG00000225968	ELFN1	extracellular leucine rich repeat and fibronectin type III d
ENSG00000137204	SLC22A7	solute carrier family 22 member 7
ENSG00000167910	CYP7A1	cytochrome P450 family 7 subfamily A member 1
ENSG00000132016	C19orf57	chromosome 19 open reading frame 57
ENSG00000168010	ATG16L2	autophagy related 16 like 2

ENSG00000162572	SCNN1D	sodium channel epithelial 1 delta subunit
ENSG00000185101	ANO9	anoctamin 9
ENSG00000183971	NPW	neuropeptide W
ENSG00000233392	LOC200772	uncharacterized LOC200772
ENSG00000118257	NRP2	neuropilin 2
ENSG00000183747	ACSM2A	acyl-CoA synthetase medium chain family member 2A
ENSG00000039068	CDH1	cadherin 1
ENSG00000198915	RASGEF1A	RasGEF domain family member 1A
ENSG00000240053	LY6G5B	lymphocyte antigen 6 family member G5B
ENSG00000167371	PRRT2	proline rich transmembrane protein 2
ENSG00000157992	KRTCAP3	keratinocyte associated protein 3
ENSG00000004777	ARHGAP33	Rho GTPase activating protein 33
ENSG00000055957	ITIH1	inter-alpha-trypsin inhibitor heavy chain 1
ENSG00000060566	CREB3L3	cAMP responsive element binding protein 3 like 3
ENSG00000118514	ALDH8A1	aldehyde dehydrogenase 8 family member A1
ENSG00000161031	PGLYRP2	peptidoglycan recognition protein 2
ENSG00000215375	MYL5	myosin light chain 5
ENSG00000084636	COL16A1	collagen type XVI alpha 1 chain
ENSG00000205639	MFSD2B	major facilitator superfamily domain containing 2B
ENSG00000174353	TRIM74	tripartite motif containing 74
ENSG00000008226	DLEC1	DLEC1 cilia and flagella associated protein
ENSG00000163082	SGPP2	sphingosine-1-phosphate phosphatase 2
ENSG00000228727	SAPCD1	suppressor APC domain containing 1
ENSG00000213759	UGT2B11	UDP glucuronosyltransferase family 2 member B11
ENSG00000111834	RSPH4A	radial spoke head component 4A
ENSG00000188779	SKOR1	SKI family transcriptional corepressor 1
ENSG00000172382	PRSS27	serine protease 27
ENSG00000167608	TMC4	transmembrane channel like 4
ENSG00000160716	CHRNA2	cholinergic receptor nicotinic beta 2 subunit
ENSG00000278771	RN7SL3	RNA component of signal recognition particle 7SL3
ENSG00000196604	POTEF	POTE ankyrin domain family member F
ENSG00000108602	ALDH3A1	aldehyde dehydrogenase 3 family member A1
ENSG00000099365	STX1B	syntaxin 1B
ENSG00000070388	FGF22	fibroblast growth factor 22
ENSG00000262484	CCER2	coiled-coil glutamate rich protein 2
ENSG00000148082	SHC3	SHC adaptor protein 3
ENSG00000102878	HSF4	heat shock transcription factor 4
ENSG00000078814	MYH7B	myosin heavy chain 7B
ENSG00000159958	TNFRSF13C	TNF receptor superfamily member 13C
ENSG00000101200	AVP	arginine vasopressin
ENSG00000166750	SLFN5	schlafen family member 5
ENSG00000123094	RASSF8	Ras association domain family member 8
ENSG00000014914	MTMR11	myotubularin related protein 11
ENSG00000251562	MALAT1	metastasis associated lung adenocarcinoma transcript 1
ENSG00000182389	CACNB4	calcium voltage-gated channel auxiliary subunit beta 4
ENSG00000059915	PSD	pleckstrin and Sec7 domain containing
ENSG00000113369	ARRDC3	arrestin domain containing 3

ENSG00000091622	PITPNM3	PITPNM family member 3
ENSG00000152503	TRIM36	tripartite motif containing 36
ENSG00000170049	KCNAB3	potassium voltage-gated channel subfamily A regulatory
ENSG00000224660	SH3BP5-AS1	SH3BP5 antisense RNA 1
ENSG00000165272	AQP3	aquaporin 3 (Gill blood group)
ENSG00000167972	ABCA3	ATP binding cassette subfamily A member 3
ENSG00000166819	PLIN1	perilipin 1
ENSG00000108465	CDK5RAP3	CDK5 regulatory subunit associated protein 3
ENSG00000215252	GOLGA8B	golgin A8 family member B
ENSG00000197124	ZNF682	zinc finger protein 682
ENSG00000163017	ACTG2	actin gamma 2, smooth muscle
ENSG00000026036	RTEL1-TNFRSF6B	RTEL1-TNFRSF6B readthrough (NMD candidate)
ENSG00000110628	SLC22A18	solute carrier family 22 member 18
ENSG00000230487	PSMG3-AS1	PSMG3 antisense RNA 1 (head to head)
ENSG00000225872	LINC01529	long intergenic non-protein coding RNA 1529
ENSG00000114841	DNAH1	dynein axonemal heavy chain 1
ENSG00000145198	VWA5B2	von Willebrand factor A domain containing 5B2
ENSG00000162004	CCDC78	coiled-coil domain containing 78
ENSG00000188385	JAKMIP3	Janus kinase and microtubule interacting protein 3
ENSG00000204323	SMIM5	small integral membrane protein 5
ENSG00000100156	SLC16A8	solute carrier family 16 member 8
ENSG00000168209	DDIT4	DNA damage inducible transcript 4
ENSG00000271816	BMS1P4	BMS1 pseudogene 4
ENSG00000179477	ALOX12B	arachidonate 12-lipoxygenase, 12R type
ENSG00000145040	UCN2	urocortin 2

transferase

notif 1

: 1

orting 1

ene

otif 16

omain containing 1

beta subunit 3

Supplementary Material for western blotting

Elucidating the role of intrinsic adenosine A1 receptors in acute alcoholism using human induced pluripotent stem cell-derived hepatocytes

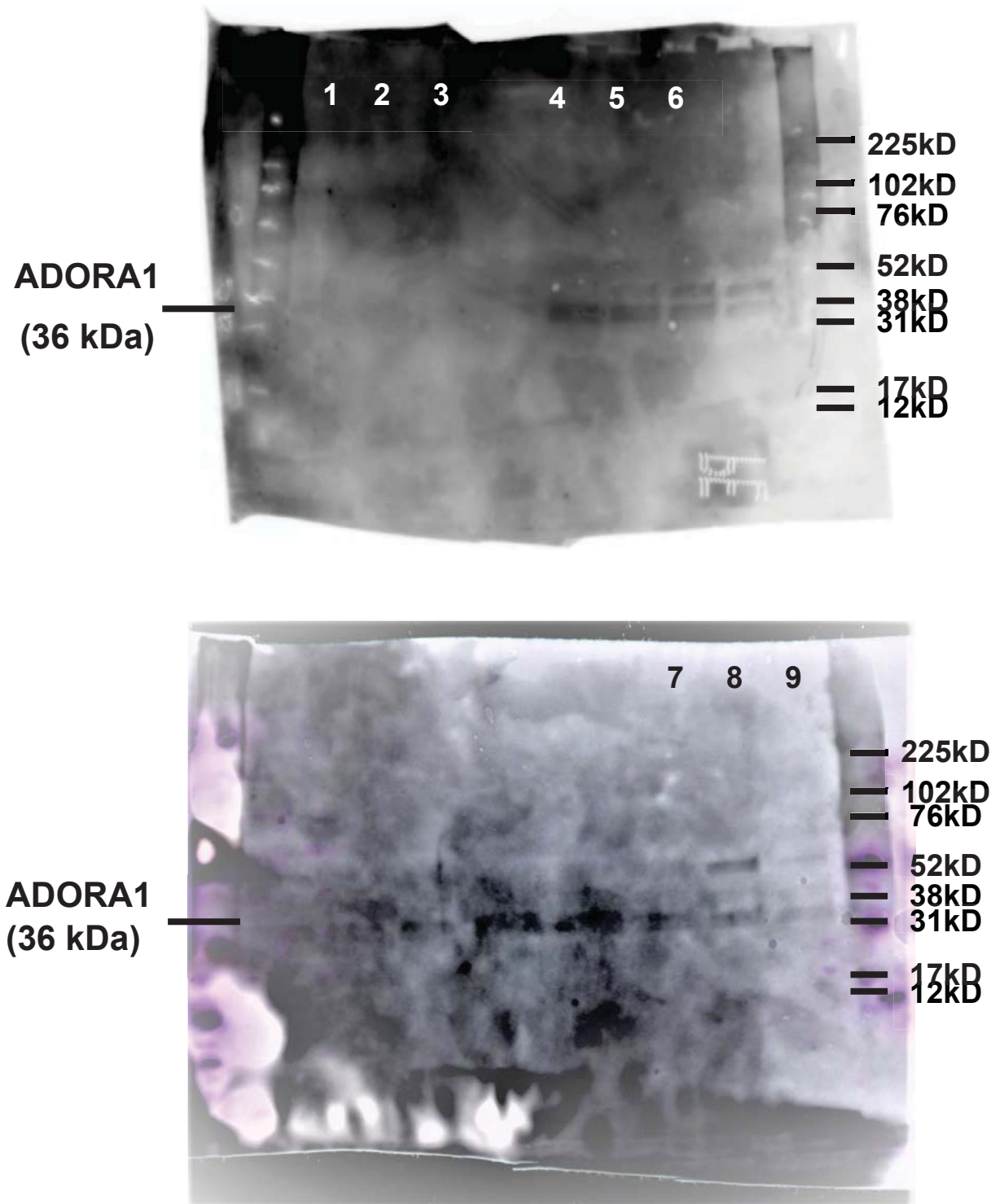
Takako Nagata, Yuning George Huang

List of material included:

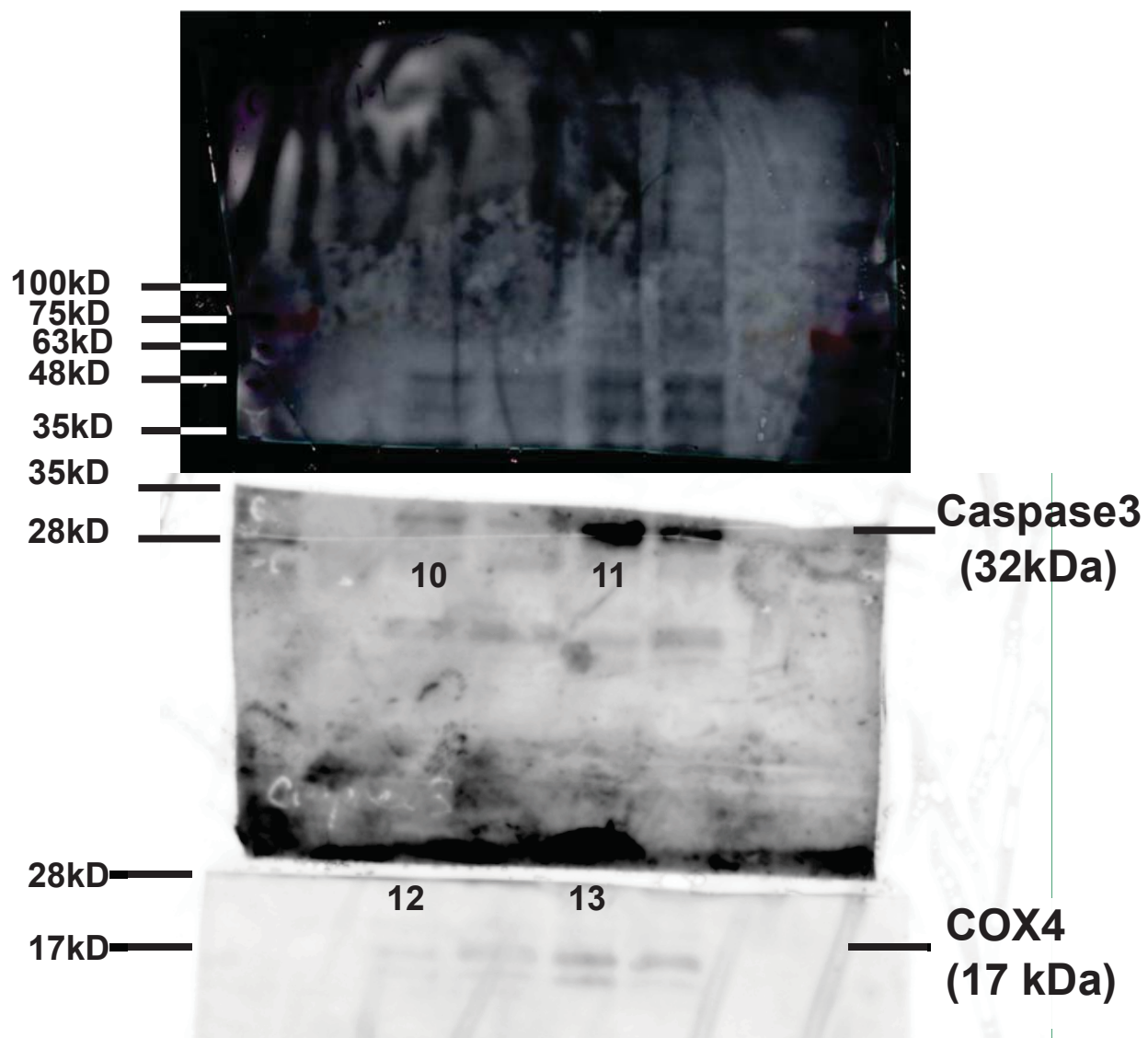
Figure S2: Unprocessed original Images of western blots

Figure S2

A



B



C

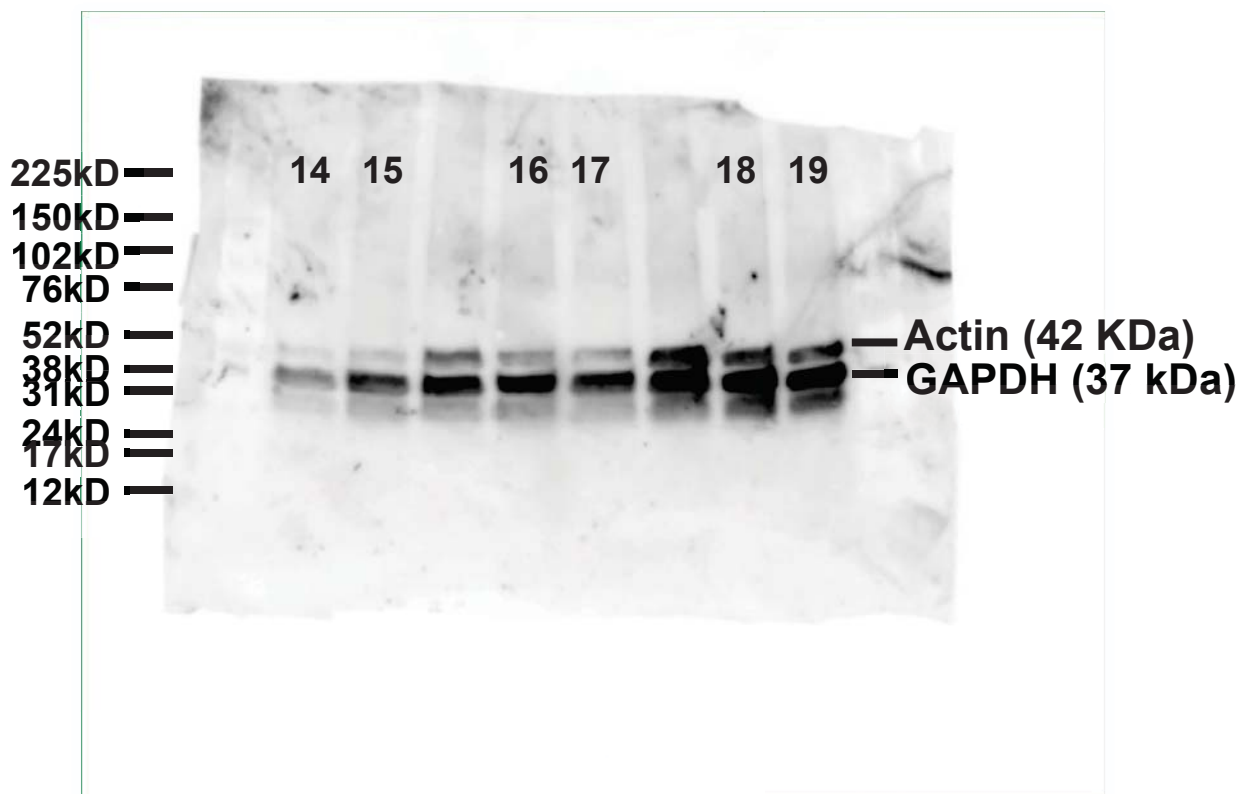


Figure S2: Original and unprocessed blots for Figure 2 and 4: (A) ADORA1 (1-3: cultured in medium only, 4-6: cultured in 100mM of ethanol, 7-9: cultured in 100mM of ethanol and siADORA1); (B) caspase 3 (10: cultured in medium only, 11: cultured in 100mM of ethanol); cox4 (12: cultured in medium only, 13: cultured in 100mM of ethanol); (C) actin and GAPDH (14-15: cultured in medium only, 16-17: cultured in 100mM of ethanol, 18-19: cultured in 100mM of ethanol and siADORA1).